FIRE FIGHTER'S EXPOSURE STUDY

K.W. Graves
Cornell Aeronautical Laboratory, Inc.

TECHNICAL REPORT
AGFSRS 71-2
December 1970

Aircraft Ground Fire Suppression and Rescue
Systems Program Office
Wright-Patterson Air Force Base, Ohio

Unclassified
Security Classification

DOCUMENT CONTROL DATA - R & D

(Security classification of title, body of abstract and indexing annotation must be entered when the overall report is classified)

1. ORIGINATING ACTIVITY (Corporate author)	2a. REPORT SECURITY CLASSIFICATION
Cornell Aeronautical Laboratory, Inc.	Unclassified
	2b. GROUP N/A

3. REPORT TITLE

Fire Fighter's Exposure Study

4. DESCRIPTIVE NOTES (Type of report and inclusive dates)

Final Report

5. AUTHOR(S) (First name, middle initial, last name)

Kenneth W. Graves

6. REPORT DATE	7a. TOTAL NO. OF PAGES	7b. NO. OF REFS
December 1970	77	11

8a. CONTRACT OR GRANT NO.	9a. ORIGINATOR'S REPORT NUMBER(S)
F33615-70-C-1715	AGFSRS 71-2
b. PROJECT NO. N/A	
c. N/A	9b. OTHER REPORT NO(S) (Any other numbers that may be assigned this report) HM-2972-Z-1
d. N/A	

10. DISTRIBUTION STATEMENT

Distribution of this document is unlimited.

11. SUPPLEMENTARY NOTES	12. SPONSORING MILITARY ACTIVITY
N/A	Tri Service System Program Office for Aircraft Ground Fire Suppression and Rescue, SMF, Wright-Patterson AFB, Ohio 45433

13. ABSTRACT

Experimental fires from pools of burning aircraft fuels were instrumented with heat meters to determine heat flux distributions for application to the design of protective clothing for firefighting personnel. The spectral distribution of infrared radiation emitted by fires was also measured. Conditions affecting the fires and the resulting heat effects that were studied were wind velocity, fuel pool area, time of burning, orientation around the fire relative to wind direction, distance from the fire, and an extraneous object in a fire. Heating rates within the fire were found to be a maximum of 8.0 cal/cm^2-sec. Because this imposes an extreme and impractical restriction upon clothing design and because the convective heating mode was significant only in a downwind direction from fires, it was concluded that radiative heating was the predominant mode that determines clothing design requirements for fire proximity. The maximum value of this heating that would be encountered for a fire of large extent was estimated at 1.9 cal/cm^2-sec. A means by which evaluation of reflective clothing can be made is described. (U)

DD FORM 1 NOV 65 1473

Unclassified
Security Classification

14. KEY WORDS	LINK A		LINK B		LINK C	
	ROLE	WT	ROLE	WT	ROLE	WT
Aircraft fuel fires						
Aircraft ground fires						
Characterization of pool fires						
Radiation from pool fires						
Convective heating near fires						
Intensity of heat near pool fires						
Spectral radiation from hydrocarbon flames						
Opacity of hydrocarbon pool fires to radiation						
Firefighter's protective clothing requirements						
Evaluation of heat reflective clothing						

FIRE FIGHTER'S EXPOSURE STUDY

K.W. Graves
Cornell Aeronautical Laboratory, Inc.

TECHNICAL REPORT
AGFSRS 71-2
December 1970

Aircraft Ground Fire Suppression and Rescue
Systems Program Office
Wright-Patterson Air Force Base, Ohio

TABLE OF CONTENTS

FOREWORD

This program was conducted under Contract No. F33615-70-C-1715 by Cornell Aeronautical Laboratory, Inc. (CAL) of Buffalo, New York for the Aircraft Ground Fire Suppression and Rescue SPO (AGFSR). Mr. Marvin Tyler, SMF, was program monitor for the AGFSR SPO and technical supervision at CAL was provided by G. A. Sterbutzel. This report, No. AGFSRS 71-2, covers research for the period July to November, 1970.

Acknowledgement is made to Messrs. T. Maj and C. M. Bork, who assisted in the conduct of the experiments.

ABSTRACT

Experimental fires from pools of burning aircraft fuels were instrumented with heat meters to determine heat flux distributions for application to the design of protective clothing for firefighting personnel. The spectral distribution of infrared radiation emitted by fires was also measured. Conditions affecting the fires and the resulting heat effects that were studied were wind velocity, fuel pool area, time of burning, orientation around the fire relative to wind direction, distance from the fire, and an extraneous object in a fire. Heating rates within the fire were found to be a maximum of 8.0 cal/cm^2-sec. Because this imposes an extreme and impractical restriction upon clothing design and because the convective heating mode was significant only in a downwind direction from fires, it was concluded that radiative heating was the predominant mode that determines clothing design requirements for fire proximity. The maximum value of this heating that would be encountered for a fire of large extent was estimated at 1.9 cal/cm^2-sec. A means by which evaluation of reflective clothing can be made is described.

LIST OF FIGURES

LIST OF FIGURES (con't)

LIST OF TABLES

NOMENCLATURE

A	Area
d	Diameter
E	Electromotive force or voltage
F	Form factor defining geometry of radiative interchange
N(λ, T)	Normal spectral intensity of radiation
q	Heat flux
R	Radius
S	Thickness
T	Temperature
t	Time
W(λ, T)	Total spectral intensity of radiation
X	Distance
ρ	Reflectivity
λ	Wavelength
ϵ_λ	Spectral emittance
μ	Microns
τ	Time response

I. INTRODUCTION

The effectiveness of protective garments for fire fighting and rescue personnel can be improved significantly by complete knowledge of the actual exposure conditions to be encountered during fire fighting operations. The thermal effects imposed upon the user must be reduced to a safe level without sacrificing mobility. Without benefit of knowledge of exposure conditions, overdesign for heating loads is likely. Existing protective clothing is bulky and lacks durability. Thermal protection may be adequate, but in a new design the same level of effectiveness probably could be preserved while simultaneously improving the flexibility or pliability of the fabric and reducing the overall weight of the garment.

The purpose of the research described in this report was to characterize the environment of jet and aviation fuel fires and produce information in a form useful to designers of protective clothing. Therefore, total heating effects in the vicinity of fires were measured, as well as the distribution of energy radiated from fires over the most significant portion of the infrared spectrum. The influence of the conditions most significant to fires is developed as a result of the experiments. These include wind velocity, ground conditions, orientation relative to wind direction, and distance from the fire. In the following sections of this report the experimental apparatus is described, and the chief points considered in selecting instrumentation for application to this research are discussed. Results of the experiments are presented and discussed relative to their significance to protective clothing.

II. EXPERIMENTAL PROGRAM

The basic approach to the characterization of fires that was assumed for this program was one of identifying the more important conditions among those affecting fires and the significant range of values for parameters describing these conditions and the fires. This facilitated the choice of instrumentation and promoted efficiency in planning. It was recognized that it was impractical to attempt complete determinations of all parameters defining fires because the number of combinations of these factors and their variations is extremely large. Therefore, a series of fires was planned around the most important conditions and a test matrix was designed in which each factor was included but not necessarily in combination with all other factors.

The most important factors relating fires and personnel exposure were considered to be: area of spread of the fire, ground surface type, time to maximum rate of burning, wind velocity, orientation relative to the fire in terms of wind direction (upwind, downwind, etc.) and distance from the edge of the fire for each fuel type. Conditions of secondary importance to the experimental program include shape of the fuel pool, extraneous objects within the fire, weather, ambient temperature, and humidity. The characteristics for defining fire effects that were deemed most important were total heating rates incident upon surfaces in the vicinity of fires and the nature of the spectrum of infrared radiation, which constitutes all the energy incident upon objects located outside the path of the flames. Flame temperatures and visual appearance of the flames were considered to be incidental characteristics.

A site was prepared for burning liquid fuels by imbedding circular steel rings in a level, flat concrete pad. The rings thereby provided an enclosure for liquids. Heat meters were arranged in the vicinity of the fire at heights of 6 ft. or less above ground for providing a continuous record of total heating rates. Heat meters were arranged in four circles around the fire site. Each circle was a different diameter. The smallest was either the same as the pool diameter or only a few feet larger, and the others were progressively

larger. See Table I for actual diameters for each pool size. The meters were placed so that they formed, roughly, three lines extending radially from the center of the fire site. Usually, one line consisting of four meters was directed downwind, one with three meters extended 90 degrees to the side and the rest formed a line directed upwind. It was not always possible to follow the wind direction by moving the heat meter stands around because of the wires so that during a few fires the upwind readings were not obtained. (Fires No. 6, 7, and 14.) A typical arrangement of meters around a fire is shown in Figure 1. Infrared radiation of the flames at six different wavelengths was detected by radiometers located about 50 ft. from the fire site.

A complete list of all fire tests conducted is given by Table II. The conditions for each fire are noted, including pool diameter, fuel type, wind velocity, type of ground surface, and weather conditions. Three types of aircraft fuel were burned: JP-4 and JP-5 jet fuels and aviation gasoline (Avgas). Sufficient fuel was burned during each fire to permit it to reach maximum intensity and burn at that rate for at least one minute and usually two, to permit satisfactory recording of data.

Air contamination measurements were made in the vicinity of flames from these fires after completion of the heat intensity experiments, as shown by Table II.

TABLE I

HEAT METER DISTANCE FROM FIRES
(From Edge of Pool)

Pool Diameter, ft.	3	6	12	18 2/3
	0	0	3.0	4.0
	1.5	3.0	6.0	9.0
	3.5	7.0	12.0	16.0
	6.0	12.0	20.0	24.0

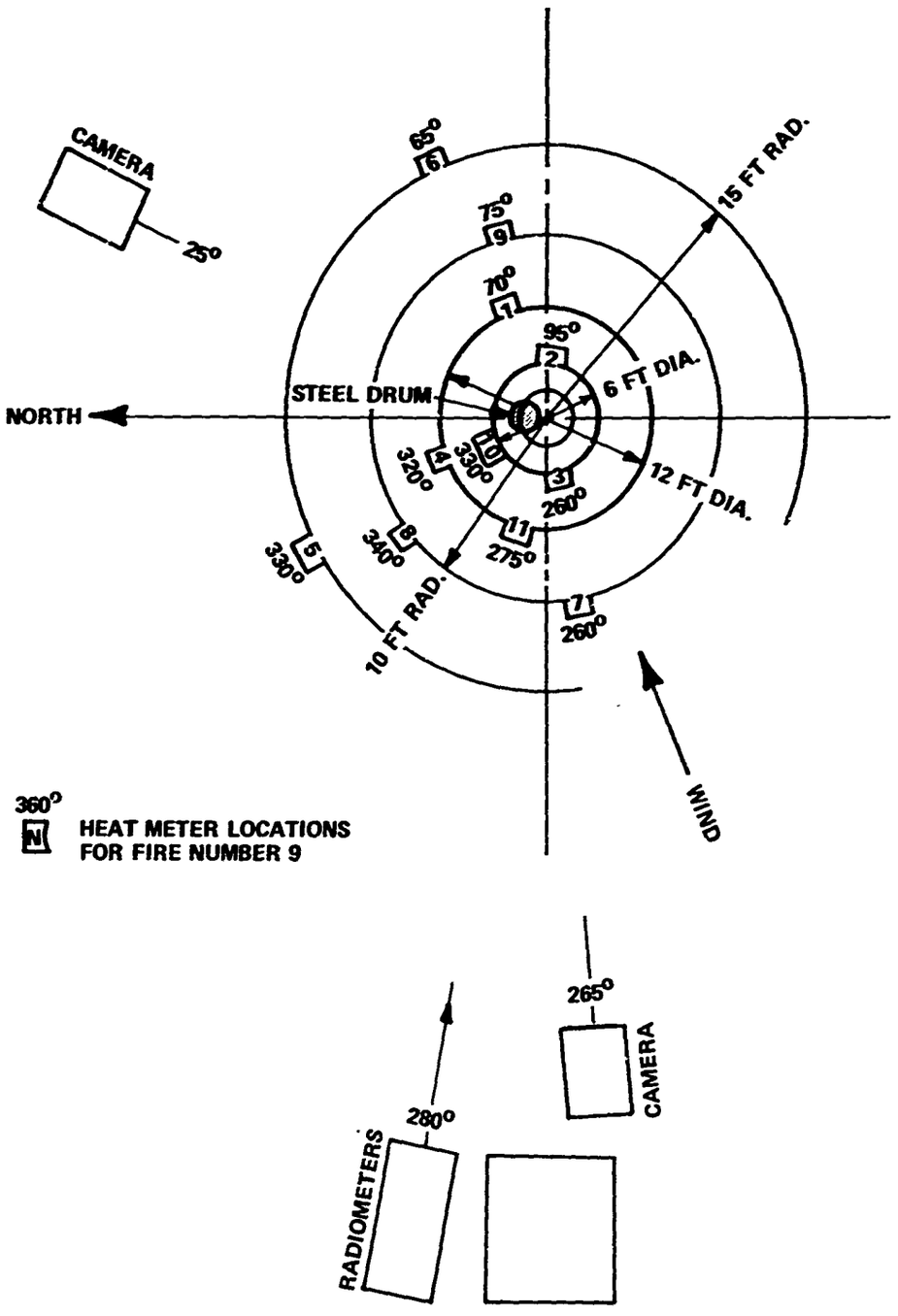

Figure 1 TYPICAL LAYOUT OF FIRE SITE & INSTRUMENTATION

TABLE II

FIRE TEST RESUME'

Test No.	Pool Dia.	Fuel	Wind mph	Wind Dir.*	Ground Cond.	Heat Mtr. Ele.	Weather	Extra. Mat'l	Extng. Agent	Rel. Hum. %	Amb. Temp. °F	Remarks
1	6	JP-5	10-15	NW-off	water	level	clear	none	none	-	70	No T/C's (thermocouples)
2		JP-5	5-10 10-20	SW-on						70	81	0-2 min. 2-4 min.
3		JP-5	5-10	SE-on						69	76	No T/C's
4		JP-4	5-10	SE-off						69	80	No T/C's
5		JP-4	15-19	SW-off	con-crete				water spray	75	65	No radiometer data.
6		JP-5	3-5	S-on	con-crete		cloudy		water spray	90	50	
7		JP-5	2-5	S-off	water				none		51	
8		JP-4	4-8	W-on					3% pr. foam		51	
9		JP-5	15-20	W-on				55-gal. drum	water spray		52	Fire slow to spread, required 2 min. No flames between radiom's & drum.
10		JP-5	5-9	W-off		sloping		none	w.spray	70	60	
11		JP-5	1-2	SE-on	earth	level	clear		none	60	70	
12		Avgas	3-5	SE-on	water					60	70	
13		JP-4	3-6	SE-on						55	70	
14		JP-4	2-6	S-on					light water	55	62	

*Off and on refer to alignment of wind with heat meters.

TABLE II (con't)
FIRE TEST RESUME

Test No.	Pool Dia.	Fuel	Wind mph	Wind Dir.*	Ground Cond.	Heat Mtr. Ele.	Weather	Extra. Mat'l	Extng. Agent	Rel. Hum. %	Amb. Temp. °F	Remarks
15	6	Avgas	1-4	W-on	water	level	clear	none	none	55	65	
16	6	JP-5	2-6	W-on	earth	sloping	clear			55	63	
17	3		0-3	NE-on	water	level	cloudy			87	67	
18	12		3-7	NE-on			cloudy			87	67	
19	12		7-10	E-on			clear			80	55	
20	12		14-18	E-on			clear			80	53	
21	18'8"		2-3	N-on			cloudy			93	50	
22	6		3-5	N-on						93	50	
23		JP-4	1-3	N-on					light water	97	49	
24			7-9	N					none	97	49	Gas sampling test - No radiometer or heat meter data taken.
25			8-11	SW							53	" " " "
26		JP-5	8-11	SW							50	" " " "
27		JP-4	8-10	W							44	" " " "
28		JP-4	8-10	W							44	" " " "

III. EXPERIMENTAL PROCEDURE

Radiometer Calibration

Calibration of radiometer detector and filter combinations was conducted by the following procedure: (See Figure A2, Appendix)

1. Set oven power and allow it to stabilize.
2. Mount filter in its holder. Place detector to be calibrated at image plane. Connect detector to its voltage box and amplifier .
3. With lights out, check output of cell to be sure the limit of 1.5 times 50 mv/bias volt is not exceeded.
4. Put thermopile in place and observe oven stability. When settled, record the thermopile output. Quickly replace it with the detector-adjust position for max output after starting the chopper. Then run oscillograph to get trace for detector. Block optical path for zero output trace. Record amplification factors for both the thermopile and the detector.
5. Repeat Step 4 at lower oven setting.
6. Repeat whole procedure for another combination of detector and filter.

Fire Test Procedure

Initial preparations made previous to starting the fires included setting oscillograph gains for the heat meters and thermocouples, loading and adjusting cameras, adjusting and recording zero levels for all oscillograph traces, and checking for wind velocity and direction. The heat meter stands were placed, and when conditions were suitable, the fuel was poured into the area enclosed by retaining rings and ignited. The ignition was easily accomplished for both JP-4 and Avgas fires, but it was necessary to use fuel-soaked paper draped over the edge of the pool at numerous places to ignite JP-5. After the entire pool became covered with flames, the oscillographs were started.

During the fire, the radiometer view was moved to the flame region of highest visual intensity near the ground (usually 5 ft. above pool level), and

a shutter was actuated intermittently to obtain a zero level of intensity. Wind velocity readings were recorded by hand at the rate of several a minute, and the cameras were triggered several times.

After the fire started to subside, the oscillographs were turned off; the time of day, ambient temperature, relative humidity, and the barometer reading were recorded.

The fuel used was procured from sources that supply the airlines and CAL for its operations of military type airplanes and was specified as aviation quality.

Gas Analysis Procedure

Samples of air in the vicinity of JP-4 and JP-5 fires were gathered in evacuated containers, three at a time through long tubes by the following procedure. Given the desired wind velocity, the containers (volume = 2/3 ft^3) were connected to a vacuum pump for evacuation, near the fire site. Each had two outlets, and the second one was connected to a sampling tube about 15 ft. long (1/4 in. copper tubing). A small amount of fuel was ignited within the 6 ft. ring of the fire site to produce smoke for assistance in proper placement of the open ends of the sampling tubes relative to the fire. When the sampling containers were evacuated, fuel was poured into the ring and ignited. The fire was allowed to reach maximum intensity, and when the flames were observed to be at the desired orientation relative to the sampling tubes, clamps were released and samples were drawn. (Fill time was only 12 sec.) After securing the fire, the samples were cool enough for analysis. The large sample volume taken was more than sufficient to permit the repeated withdrawals required for analysis of hydrocarbons, oxygen deficiency, in addition to CO_2, CO, NO, NO_2, and ozone content. The withdrawals were made by

suction using a Dräger multi-gas detector by permitting air to displace the gas taken out. Outlets led from each end of the container, which was placed upright so that the gas was taken off the bottom while the less dense air flowed in the top. The exception was carbon monoxide, which was tested first. No mixing of the inducted air occurred during the time the measurements were made. This was determined by the fact that CO_2 content remained constant during the measurement period.

IV. EXPERIMENTAL RESULTS

Results from the fire tests are presented in either graphic or tabulated form. The conditions under which each test was conducted are specified with each group of results. In addition, a complete resume of the tests conducted is given by Table II, which lists all the conditions for each fire. Almost all of the data that are presented are selective in the sense that because continuous records were obtained, they consist of an infinite quantity of detail, but it is feasible to give attention to a limited amount only. Therefore, in an effort to maximize the yield of the program, an attempt was made to give more attention to the results that were deemed to be more significant to the purpose of the program. One result of this was that some types of data from certain fires were not used. For example, heat meter and radiometer data are presented only so that comparisons can be made in terms of the conditions specified for fire tests.

Thermocouple data are presented in Table III to show the peak values for each of a number of representative fires.

Effects of the various conditions of wind velocity, fuel type, ground type, and fuel pool size upon the peak heating rate to the heat meters are shown in relation to distance from the fire in Figures 2a to 2f.

Wind Velocity

Anticipated effects of wind velocity are shown by the heat meter results (Figures 2a, 2b), namely that downwind from the fire a stronger wind tends to raise the heat intensity at a given distance away from the edge of the fuel pool. However, it appears that at 20 ft. from the fire on the 12 ft. diameter pool a reversal has occurred at above 14 mph wind velocity. The heating rate for a 10 mph wind may be near the maximum value for 20 ft. away (and an elevation of 3 ft.). The heating rate to a surface at 90° to the wind direction (off to one side) also seems to reach a maximum (at any distance)

TABLE III

THERMOCOUPLE DATA FOR FIRES

(Maximum Values Attained During Fire)

Fire No. 5 JP-4 burning on concrete 6 ft. pool diameter	15-19 mph wind
Height Above Pool in.	Temperature Over Center of Pool ~°F
11	1750
24	--
36	553
47	710
Fire No. 11 JP-5 burning on earth 6 ft. pool diameter	**1-2 mph wind**
11	1900
24	2020
36	1830
47	1600
Fire No. 13 JP-4 burning on water 6 ft. pool diameter	**3-5 mph wind**
11	1720
24	1350
36	500
47	325

TABLE III (con't)

Fire No. 14 JP-4 burning on water 6 ft. pool diameter	2 - 6 mph wind	
Height Above Pool in.	Temperature °F at center of pool	at downwind edge
8		--
11	1170	
18		1305
24	500	
36	535	
47	450	
70		1950
Fire No. 15 Avgas burning on water 6 ft. pool diameter	**1-4 mph wind**	
8		--
11	1800	
18		1390
24	1300	
36	630	
47	400	
70		1750
Fire No. 16 JP-5 burning on earth 6 ft. pool diameter	**2-6 mph wind**	
8		--
11	1825	
18		240
24	1220	
36	770	
47	550	
70		1350

TABLE III (con't)

Fire No. 17 JP-5 burning on water 3 ft. pool diameter	0-3 mph wind	
Height Above Pool in.	Temperature °F at center of pool	at downwind edge
11	1350	
24	390	
36	140	
47	170	
Fire No. 18 JP-5 burning on water 12 ft. pool diameter	**3-7 mph wind**	
8		--
11	1550	
18		--
24	1520	
36	1150	
47	740	
70		2020

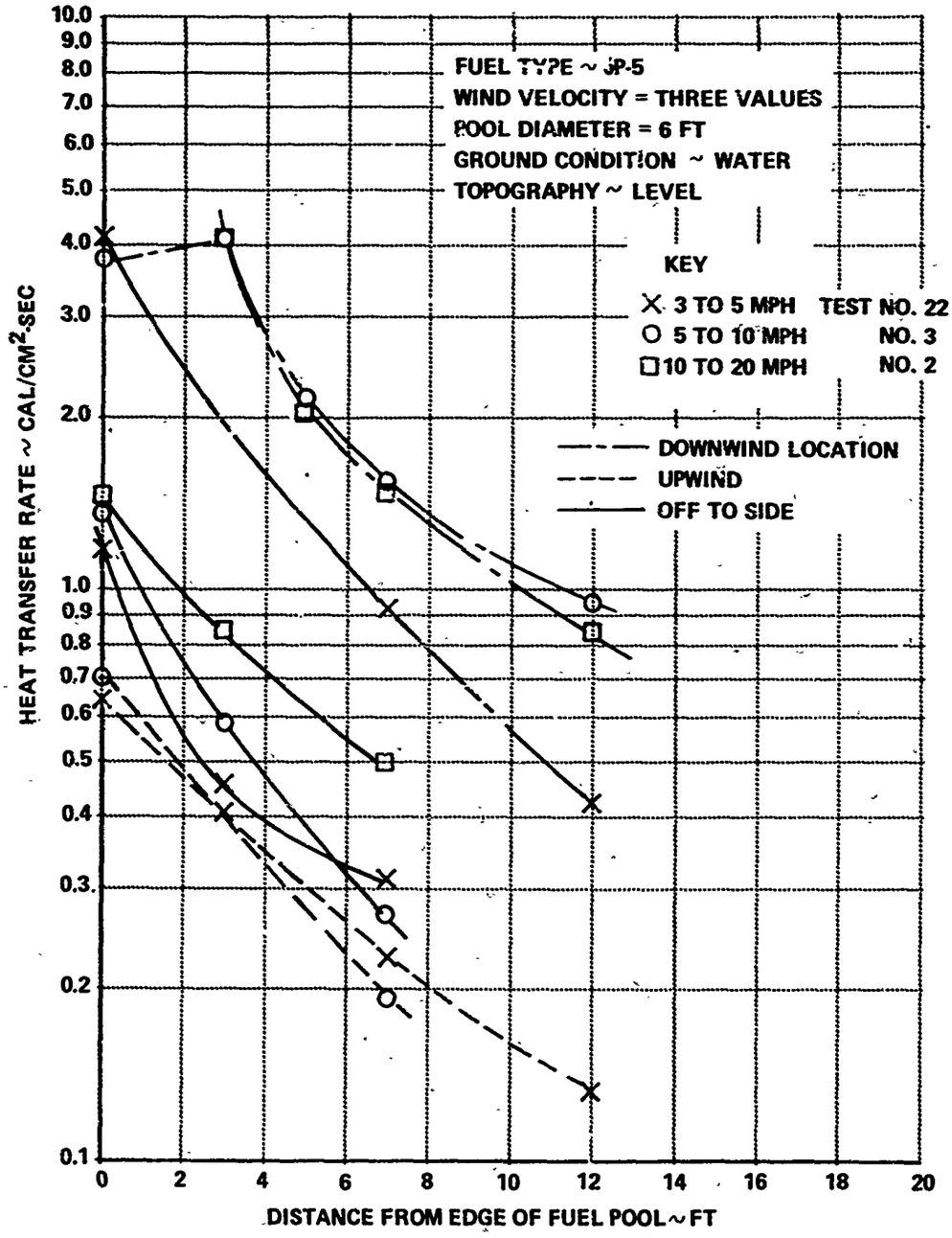

Figure 2a EFFECT OF WIND VELOCITY UPON HEATING RATE TO A SURFACE NEAR FIRE FROM BURNING AIRCRAFT FUEL

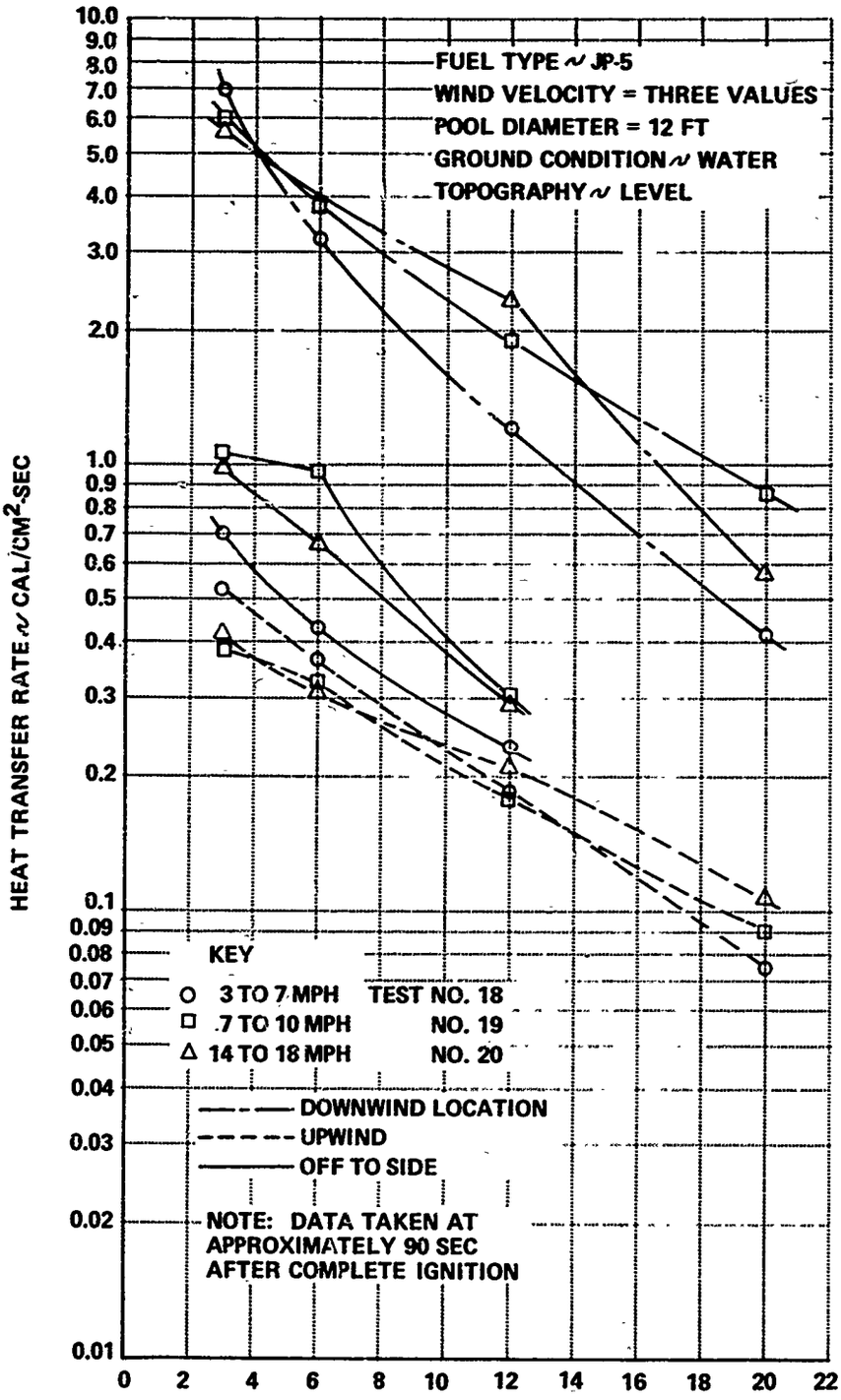

Figure 2b EFFECT OF WIND VELOCITY UPON HEATING RATE TO A SURFACE NEAR FIRE FROM BURNING AIRCRAFT FUEL

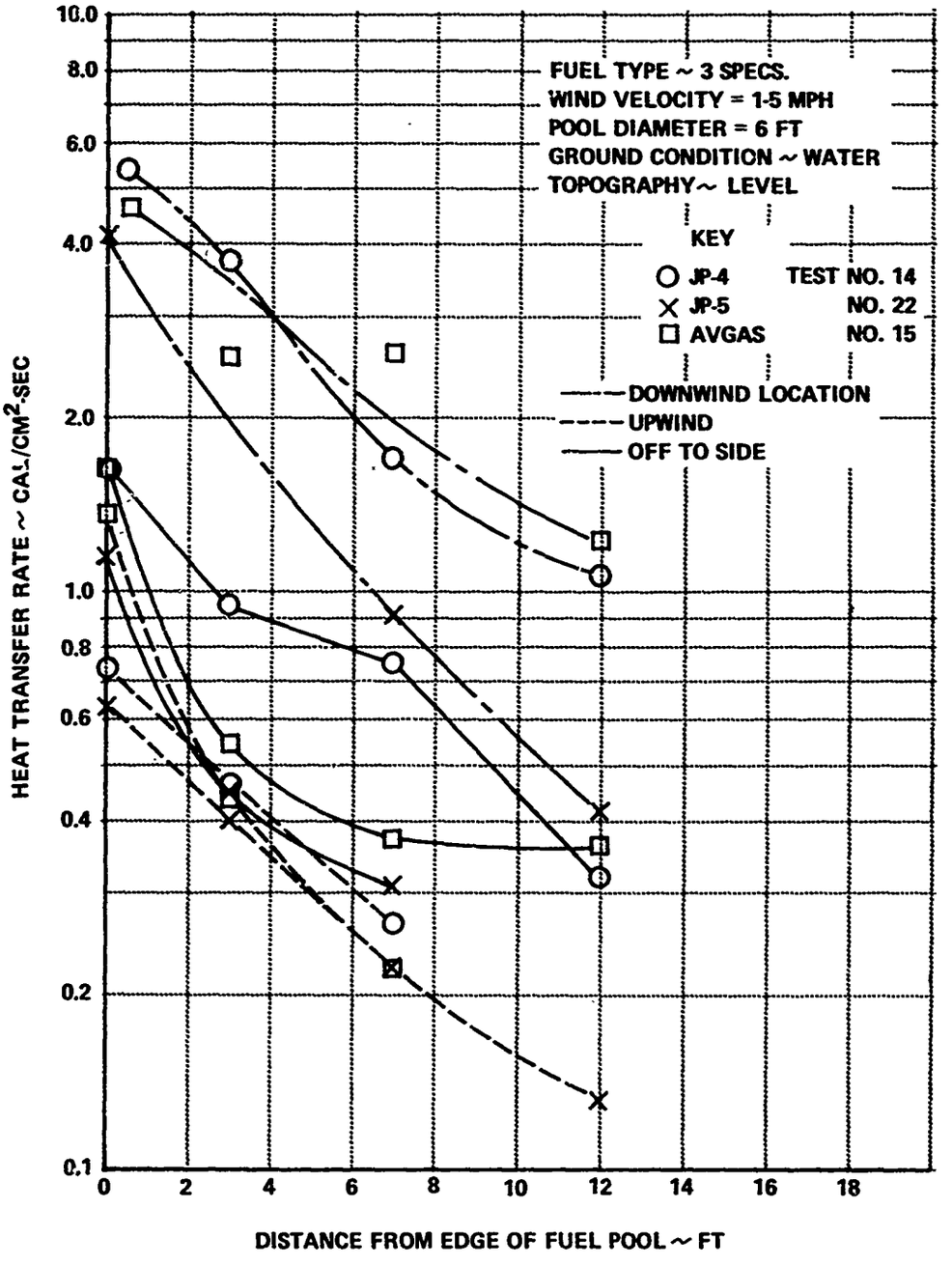

Figure 2c EFFECT OF FUEL TYPE UPON HEATING RATE TO A SURFACE NEAR FIRE FROM BURNING AIRCRAFT FUEL

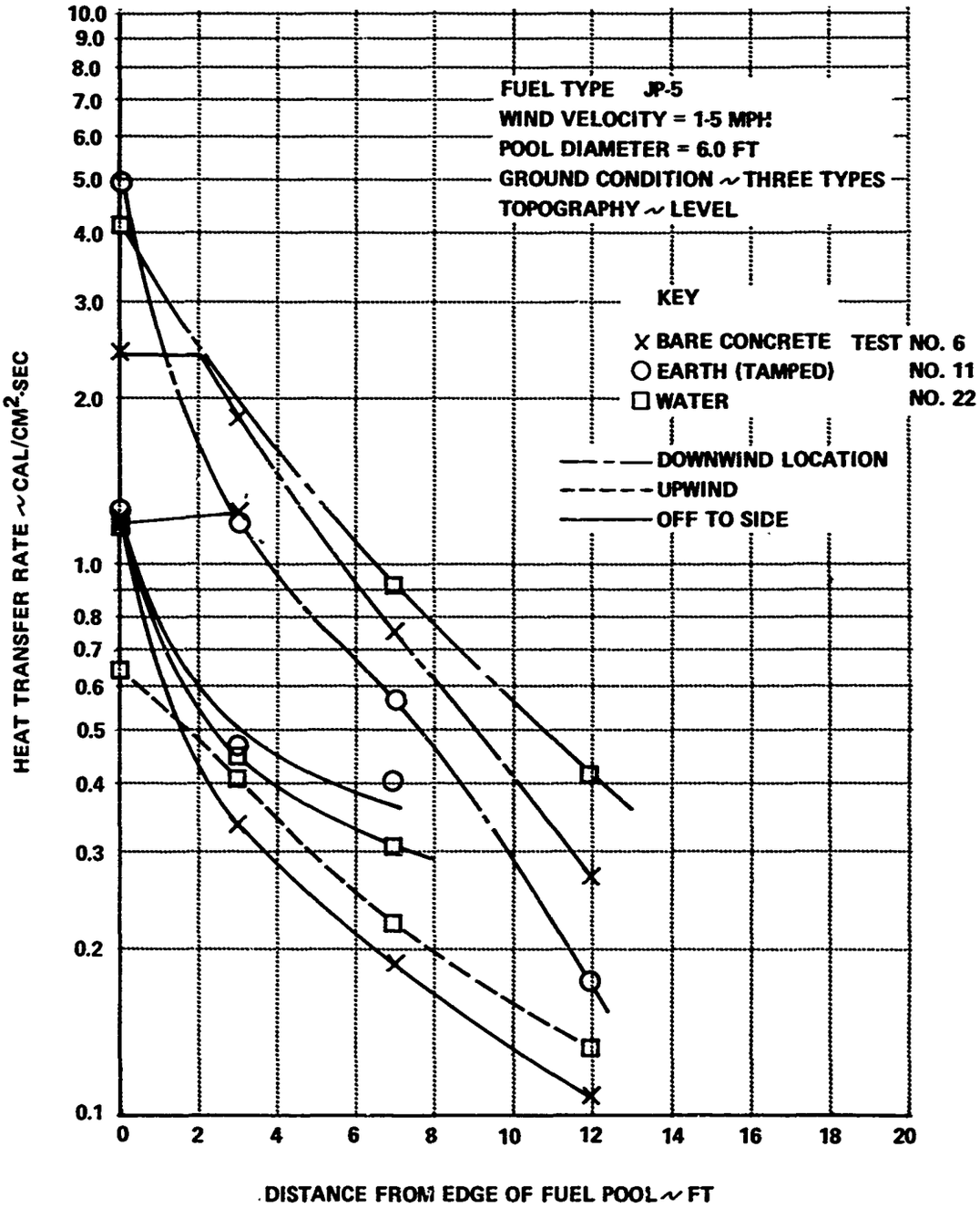

Figure 2d EFFECT OF GROUND CONDITION UPON HEATING RATE TO A SURFACE NEAR FIRE FROM BURNING AIRCRAFT FUEL

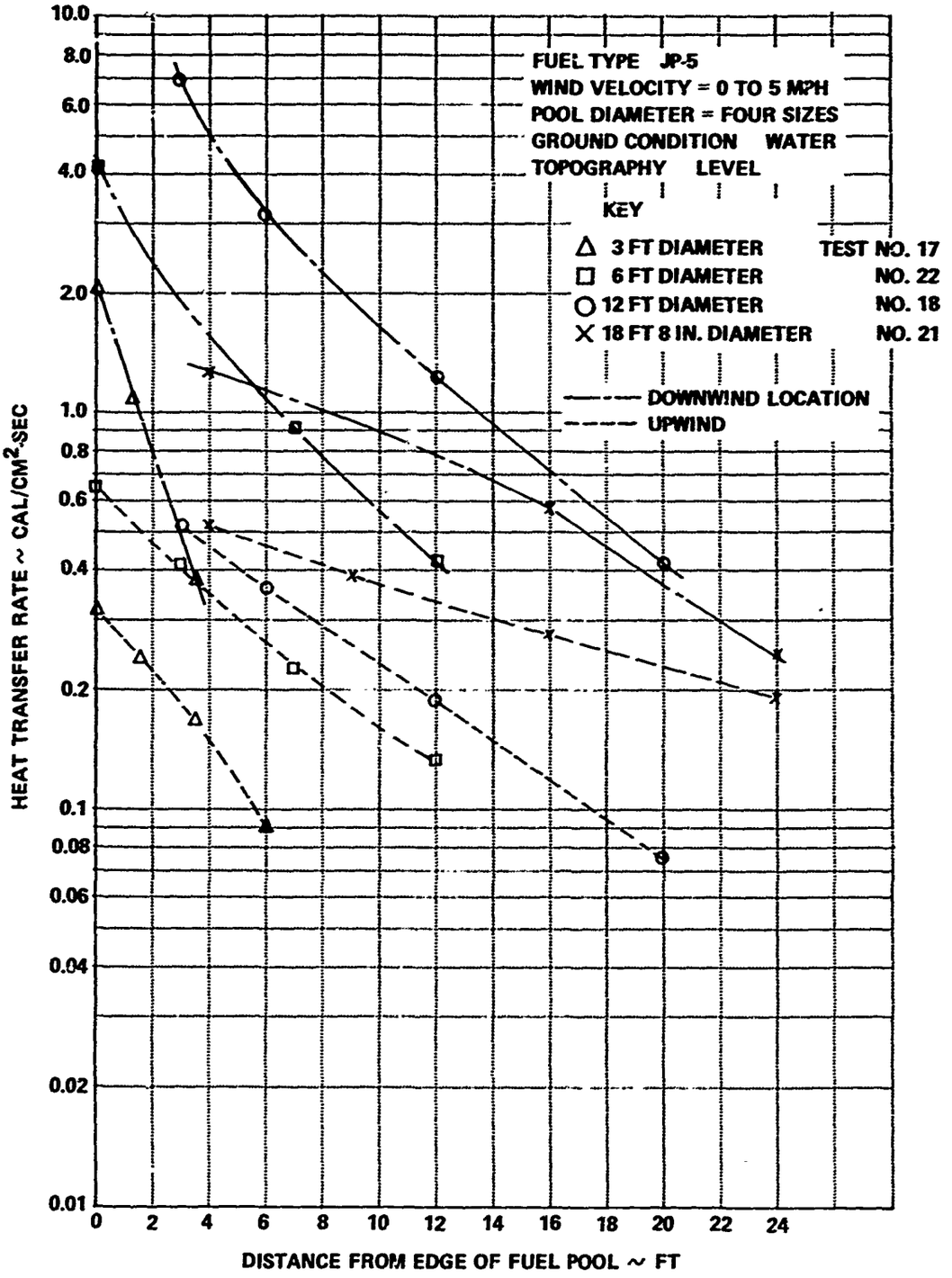

Figure 2e EFFECT OF POOL SIZE UPON HEATING RATE TO A SURFACE NEAR FIRE FROM BURNING AIRCRAFT FUEL

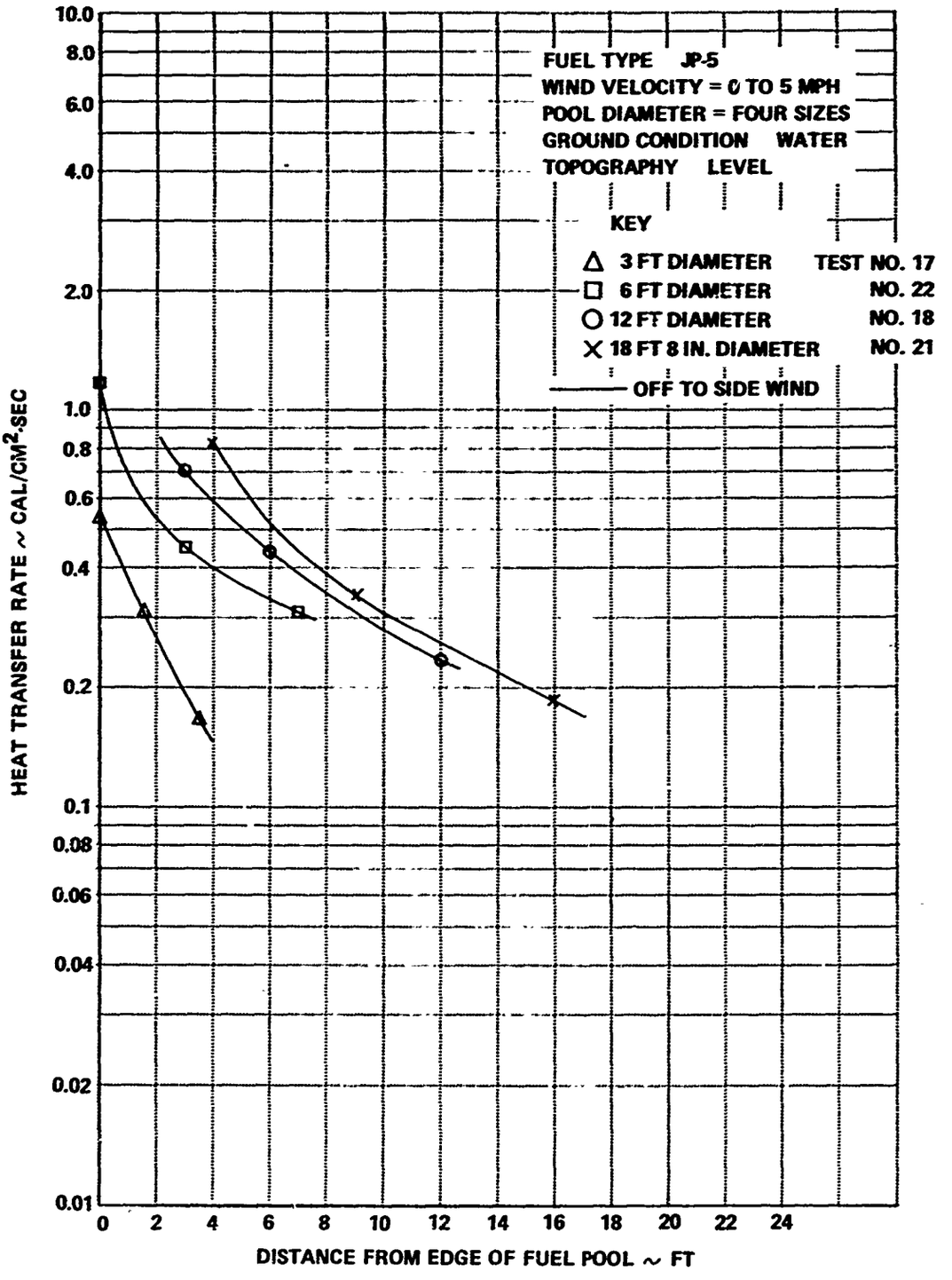

Figure 2f EFFECT OF POOL SIZE UPON HEATING RATE NEAR FIRE FROM BURNING AIRCRAFT FUEL

for the higher wind velocities. Contrary to expectations, the heating rate upwind from fires is not consistently higher when the wind velocity is low (when the bulk of the flames reaches higher and is closer).

The wind velocity readings that were recorded were instantaneous values, and provision was not made for either correlating or synchronizing them with the timing marks of the oscillographs. As a result, the exact wind velocity, at the time the peak heating was recorded, is unknown. However, it it will be shown that the behavior of averaged heat meter readings agrees with the instantaneous peak values.

In order to determine average heating rates, the heat meter traces were planimetered over a 20-sec period for several fires (Nos. 19, 20, 21, and 22). The average heating rate was equal to the measured area under each trace divided by 20 sec. Typical traces are shown in Figure 3. Average heating rates are compared with peak heating rates obtained during the 20-sec period in Figures 4a to 4d.

In general, it can be stated that average heating rates are not sufficiently different than the instantaneous peak values to affect the interpretation of results. Figure 4 shows that the major difference is the indicated level of heating rate. Most of the pairs of mating curves are parallel, and the major departures occur at the pool edge where extreme fluctuations in heating rate are typical of the fires. The nature of the fluctuations can be seen in Figure 3 for heat meters 3 ft. from the pool edge, although the magnitudes are not as great as for the edge meter. The plot of Figure 3 is a reproduction of heat meter traces for which galvanometer deflection was converted to heating rate using the proper calibration factor.

As a consequence of the above considerations, the use of an average wind velocity would be consistent with the use of averaged heating rate. It is pertinent that the median value of wind velocity between the limits quoted for each fire was found to be close to the average ($\pm$ 1/2 mph).

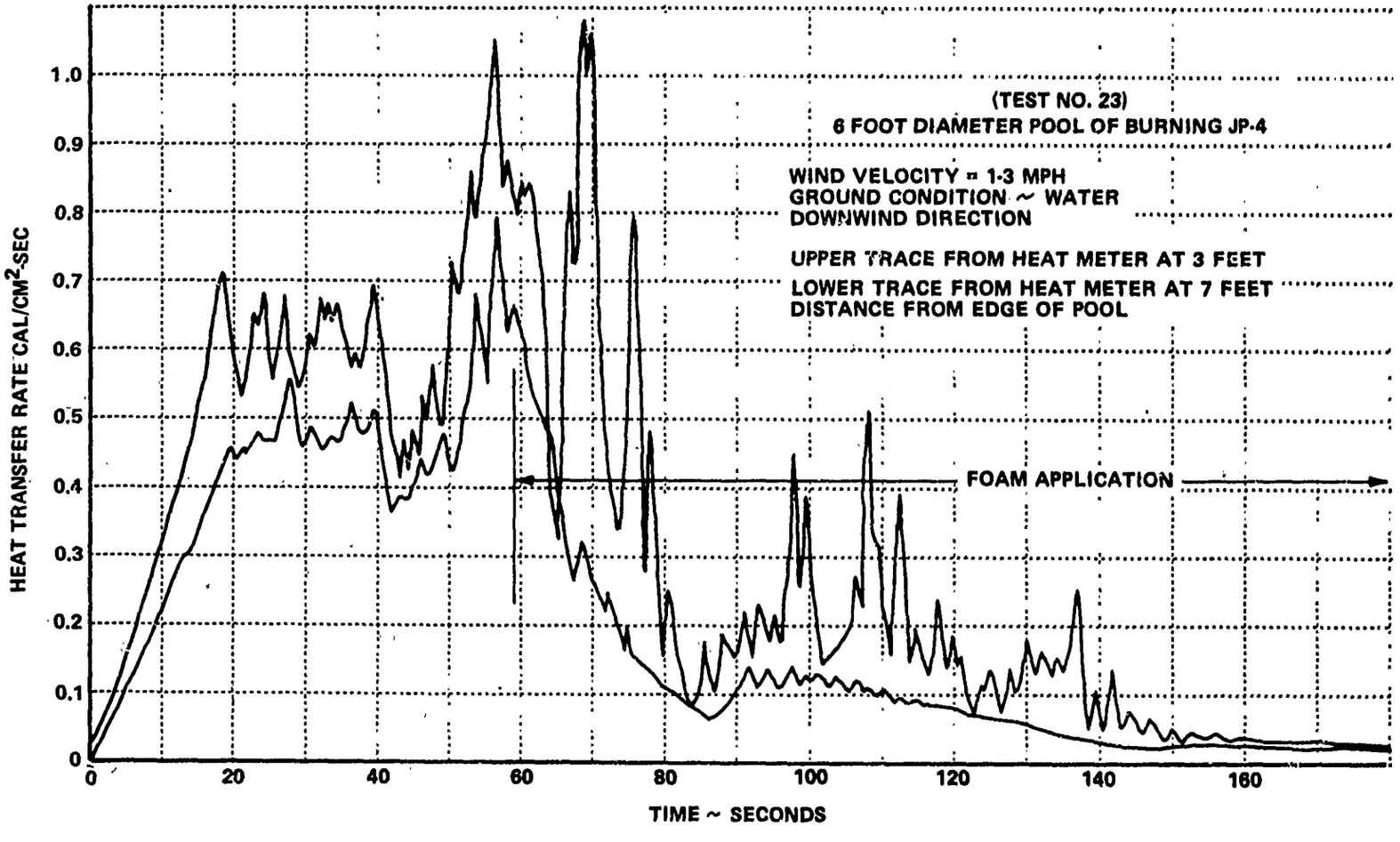

Figure 3 HISTORY OF HEATING RATE

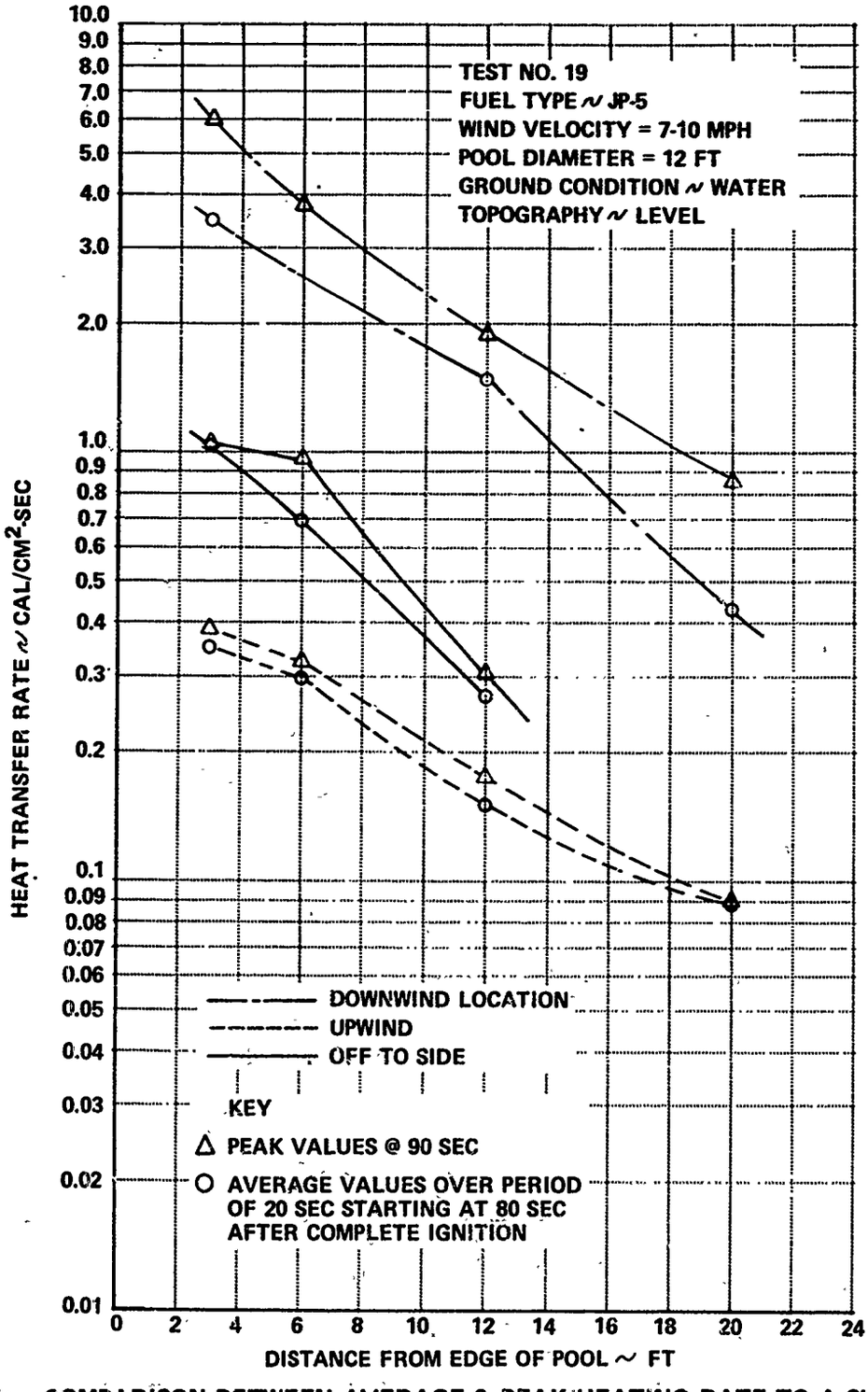

Figure 4a COMPARISON BETWEEN AVERAGE & PEAK HEATING RATE TO A SURFACE NEAR FIRE FROM BURNING AIRCRAFT FUEL

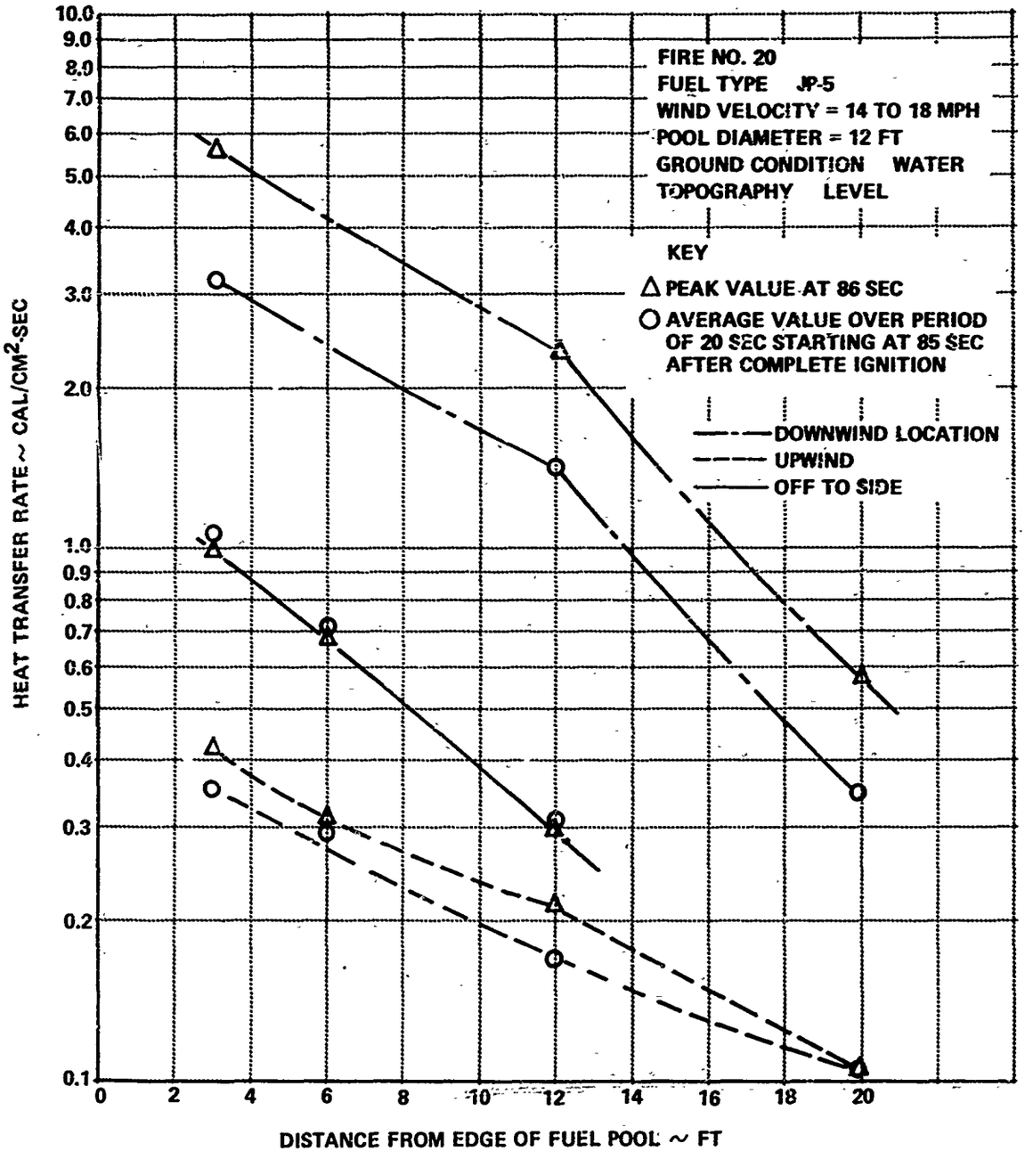

Figure 4b COMPARISON BETWEEN AVERAGE & PEAK HEATING RATE TO A SURFACE NEAR FIRE FROM BURNING AIRCRAFT FUEL

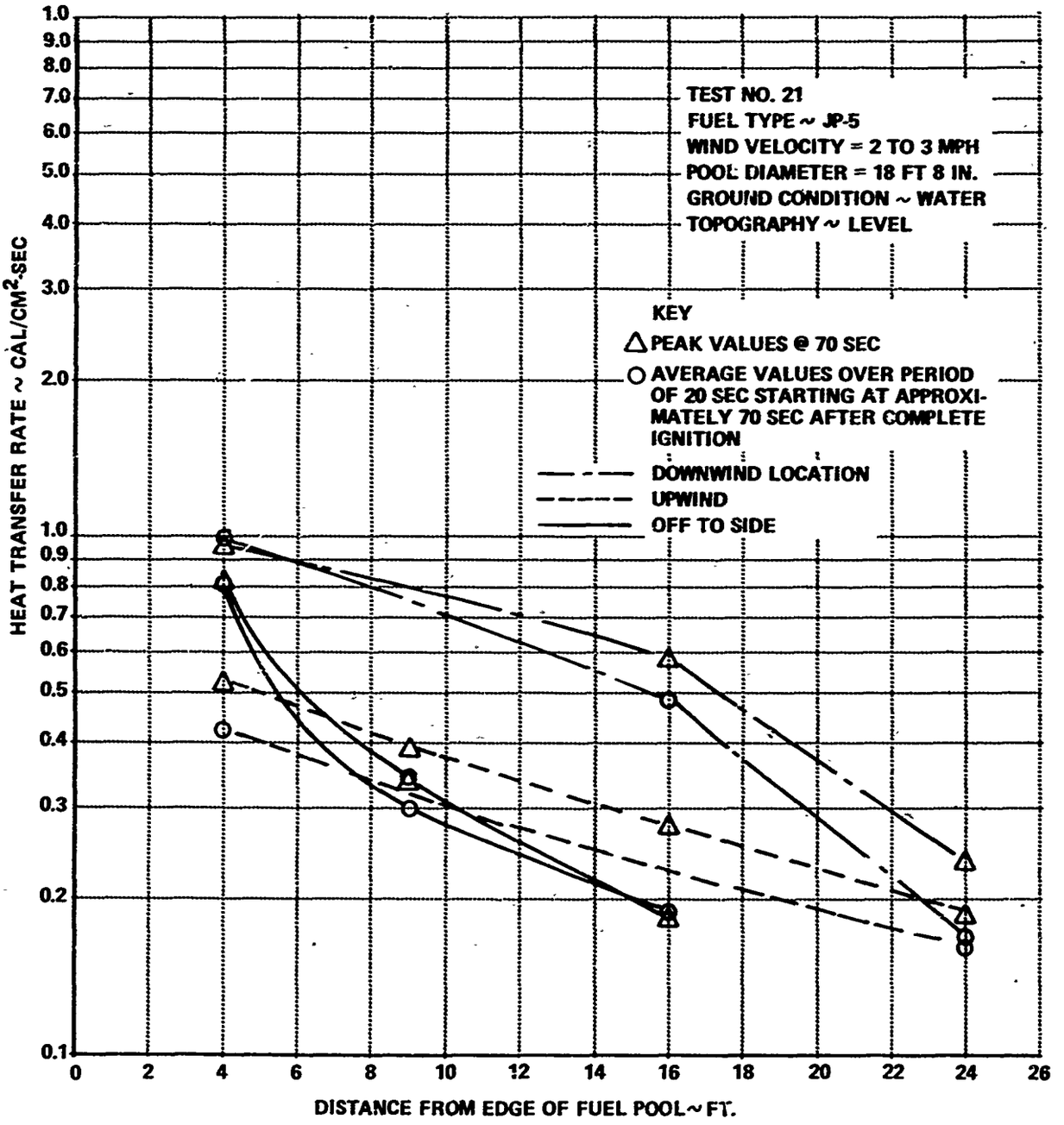

Figure 4c COMPARISON BETWEEN AVERAGE & PEAK HEATING RATE TO A SURFACE NEAR FIRE FROM BURNING AIRCRAFT FUEL

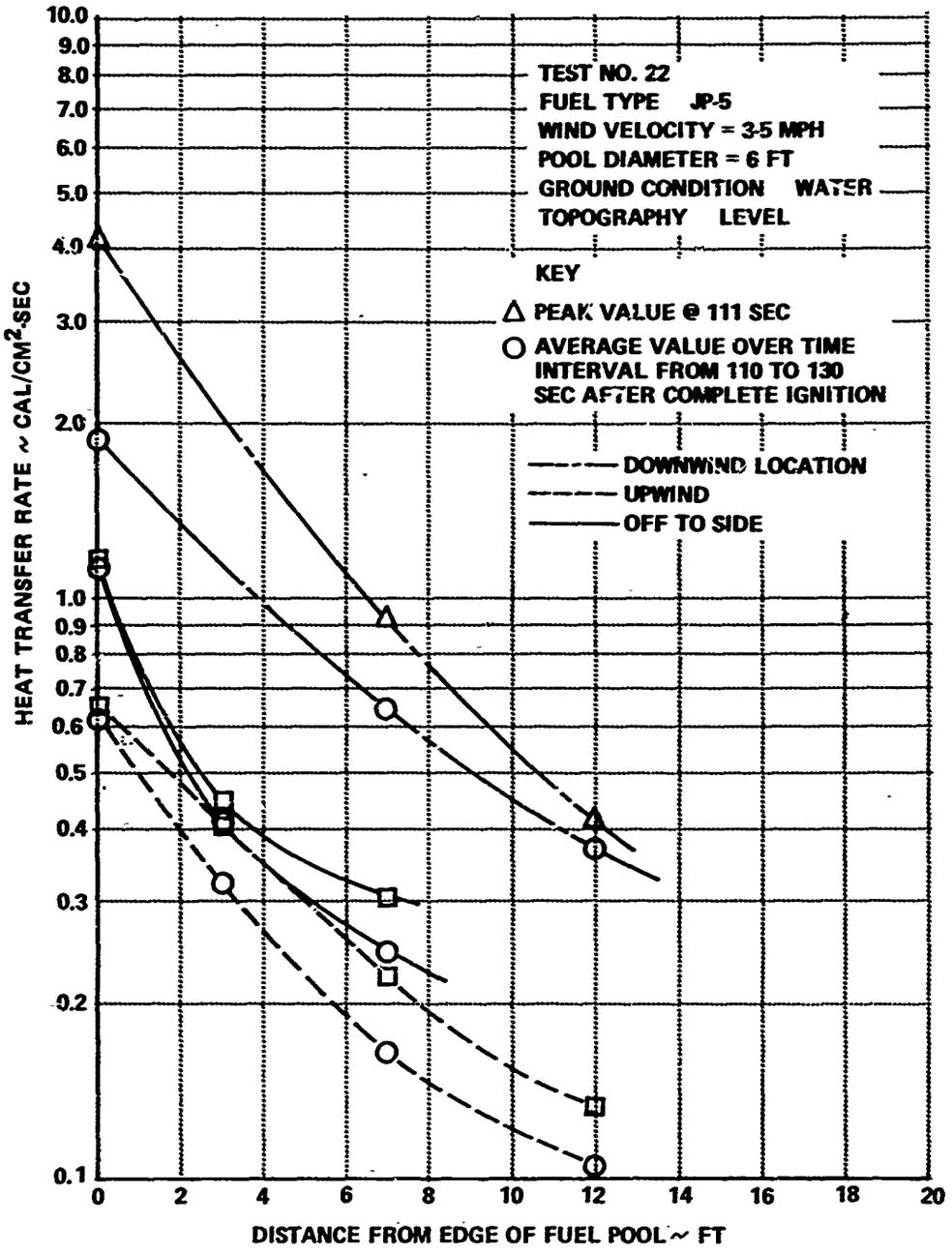

Figure 4d COMPARISON BETWEEN AVERAGE & PEAK HEATING RATE TO A SURFACE NEAR FIRE FROM BURNING AIRCRAFT FUEL

Additional information concerning the effect of wind upon fires was sought from the radiometer measurements. The spectral distribution of radiative intensity was plotted as shown in Figure 5 for the three fires on the 12 ft. diameter pool (Tests No. 18, 19, and 20). This comparison shows that there was little change in radiative intensity because of wind velocity. Note that ster. is an abbreviation for steradians of solid angle.

In this type of plot, the radiometer data are plotted as short lines, with the length of each corresponding to the half wavelength of the transmissivity curve for the respective radiometer filter and with the location relative to wavelength centered on the wavelength corresponding to the center wavelength of transmission. The amplitude of the raw data has been corrected for radiometer geometry, and its distance from the fire, to yield $N(\lambda, T)$, the energy radiated from the fire per unit of bandwidth and solid angle, and this is the form of the data plotted. It is of much more general utility than would be the raw data, which were provided as an energy flux detected for the bandwidth of the filter and the solid angle formed by the entrance aperture relative to the detector.

The distribution of radiative intensity emitted by a blackbody is superimposed upon the plot for blackbody temperatures of 1400° and 1600°K. This blackbody intensity represents the maximum possible intensity that can be radiated at any wavelength.

The photographs of Figure 6 show the apparent effect of wind velocity upon flames from JP-5 burning on water in a 6 ft. diameter pool. The wind direction was about 90° relative to a line from the camera to the pool during these fires.

Fuel Type

It was also anticipated that gasoline and JP-4 would yield more intense heating rates than JP-5. This is confirmed by Figure 2c, which compares heating rate distributions for the three fuels under very similar conditions. The only unusual characteristic of the curves is revealed by the comparison of

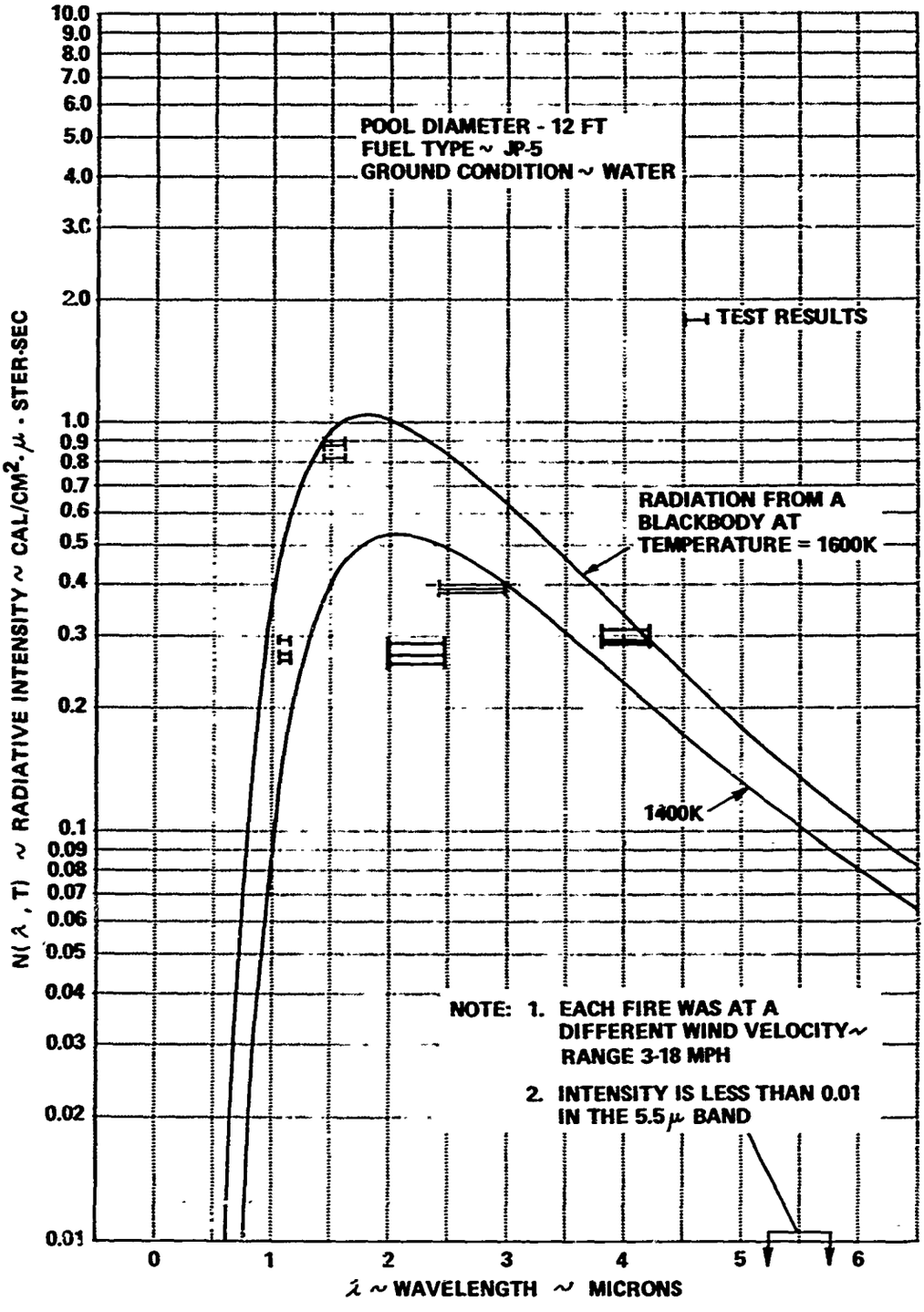

Figure 5 EFFECT OF WIND VELOCITY UPON SPECTRAL INTENSITY OF FLAME RADIATION

4 MPH
TEST NO. 16

8 MPH
TEST NO. 10

18 MPH
TEST NO. 2

Figure 6 FIRE GEOMETRY AT DIFFERENT WIND VELOCITY

heating rates off to the side for JP-4 and gasoline. It is not known why the JP-4 curve is so much higher than the curve for gasoline. The curvature for the heating rates at the side of the JP-4 fire is also much greater than for either of the other fuels. The difference in the JP-4 data does not appear to be the result of faulty instrumentation because several different heat meters were used, usually with similar results.

It is interesting to note that the radiometer measurements do not generally support a thesis that the heat intensity beyond the flames is lower for JP-5. At wavelengths of 1.1 and 2.2 microns the spectral intensity of radiation is noticeably higher (see Figure 7), and it is probable that a summation of the spectral intensity over the spectrum (on the basis of the data in Figure 7) would yield very little difference in total radiation for all three fuels. The heat meters, of course, sense radiation at all wavelengths, emitted from the whole fire, so the radiometer data are not necessarily contradictory.

A comparison can be made of the appearance of the fires for the three fuels used by referring to Figure 8. During these fires, the wind velocity was quite low (approximately 4 mph), usually blowing away from the camera.

Ground Condition

A conclusion that may be drawn from the comparison of the effect of ground conditions upon heating rate distribution is that fuel fires on either water or bare concrete are more intense than fires from liquid fuel burning on earth. See Figure 2d. A comparison of the radiometer data, Figure 9 shows that fires on water generally radiate more intensely than fires on earth and concrete, with the only significant difference occurring in the 2.2 micron band.

Fuel Pool Size

A comparison in heating rates for various fire sizes (Figure 2e) reveals no surprises except at points very close to the edge of the pool of fuel where

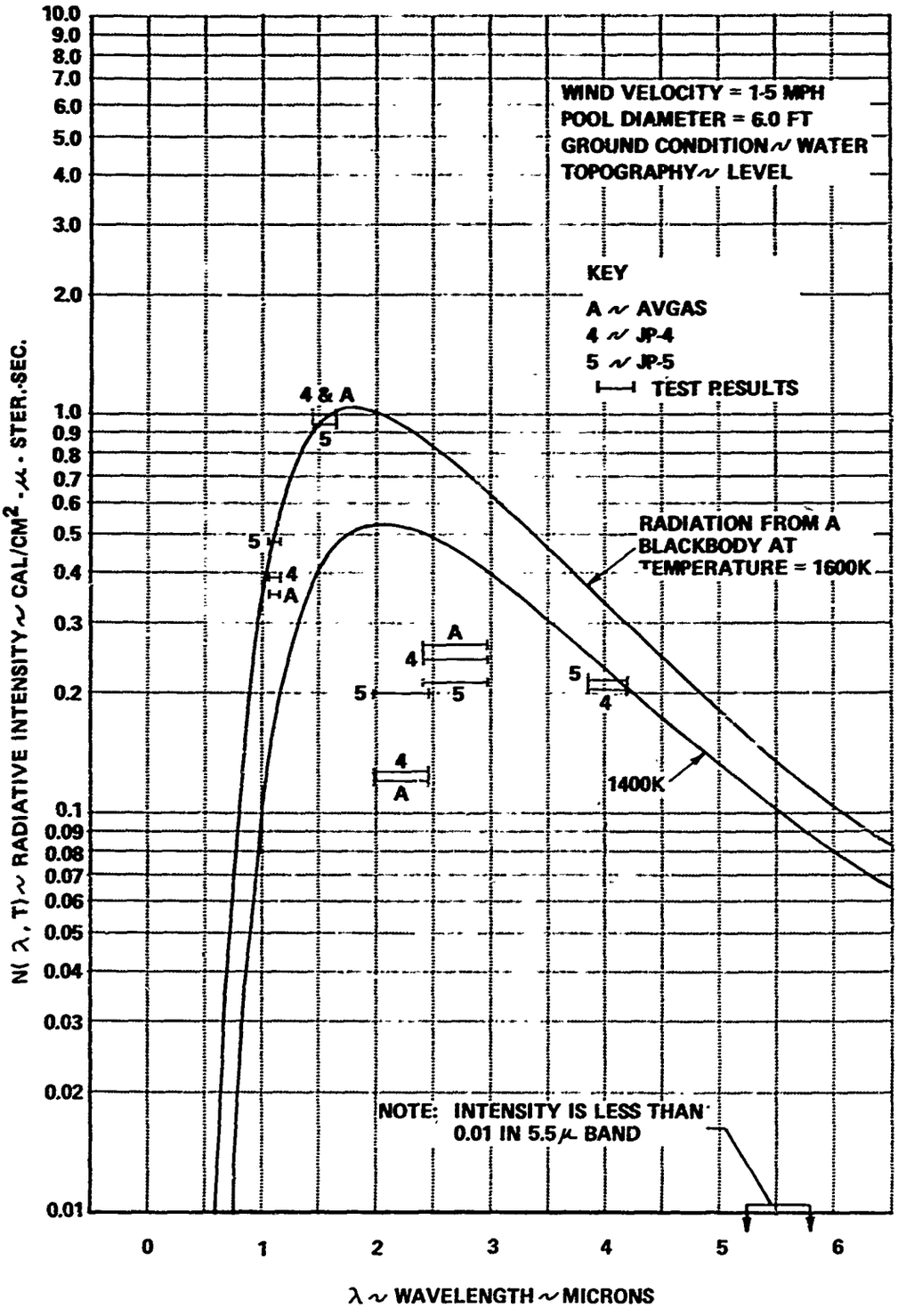

Figure 7 EFFECT OF FUEL TYPE UPON SPECTRAL INTENSITY OF FLAME RADIATION

JP-4
TEST NO. 23

JP-5
TEST NO. 6

AVGAS
TEST NO. 15

Figure 8 FIRE APPEARANCE FOR EACH FUEL

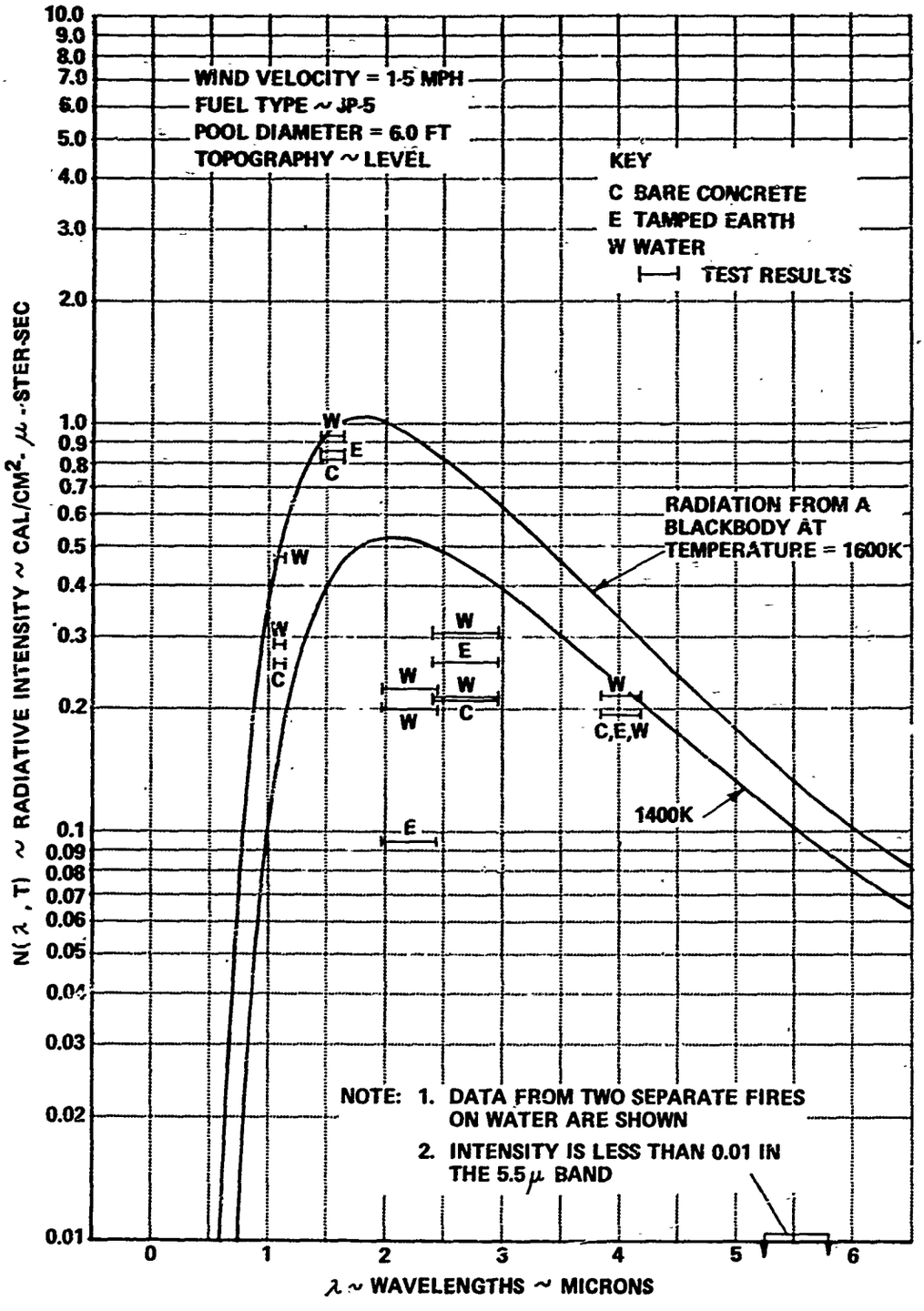

Figure 9 EFFECT OF GROUND CONDITION UPON SPECTRAL INTENSITY OF FLAME RADIATION

convection is predominant. At first observation, it may be disturbing to note that the heating rate 4 ft. downwind from the largest fire is no greater than for a 6 ft. diameter fire. However, this can be readily explained. First, this fire extended very high into the air compared to the others by virtue of its size. Any convection effects at the heat meter in question were more likely of a cooling nature rather than heating because of natural induction of air into the base of the fire (at the elevation of the heat meter). Secondly, the 12 ft. fire, for which data are plotted in Figure 2e, was conducted at an average wind velocity 3 mph higher than for the other fires, which would naturally be manifested by a downwind heating curve that would be somewhat elevated. Of special interest are the upwind heating curves, which spread farther apart as distance from the fire increases. This, of course, is an illustration of the inverse square law for radiation, or more technically speaking, the form factor for radiant interchange. The solid angle subtended by the fire and the target heat meter varies inversely as the square of distance between them and directly as fire area. For fires similar in geometry this means that radiant heating on a target 24 ft. from an 18 ft. fire would be the same as at a target 8 ft. from a 6 ft. fire. A few checks of this kind reveal that the upwind curves for the 3, 6, and 18 ft. diameter fires behave according to this law beyond a distance of one half pool diameter. Consequently, the fire diameters tested must have yielded overall fire areas in the proper ratios. A rough similarity of shapes can be seen in the photographs of Figure 10, taken from an upwind location with respect to the fires.

Radiometer data from fires of different sizes is plotted in Figure 11. It can be seen that intensity generally increases with size at the longer wavelengths. The peak intensity at 2.2 microns was reached by the 12 ft. diameter fire and at 2.7 microns the increase exhibited by the 19 ft. fire was marginal. This tends to indicate that fires of depth greater than for the 19 ft. fire would not emit much more radiative energy.

3 FEET
TEST NO. 17

6 FEET
TEST NO. 11

NOT REPRODUCIBLE

18-2/3 FEET
TEST NO. 21

Figure 10 FIRE GEOMETRY FOR DIFFERENT POOL DIAMETERS

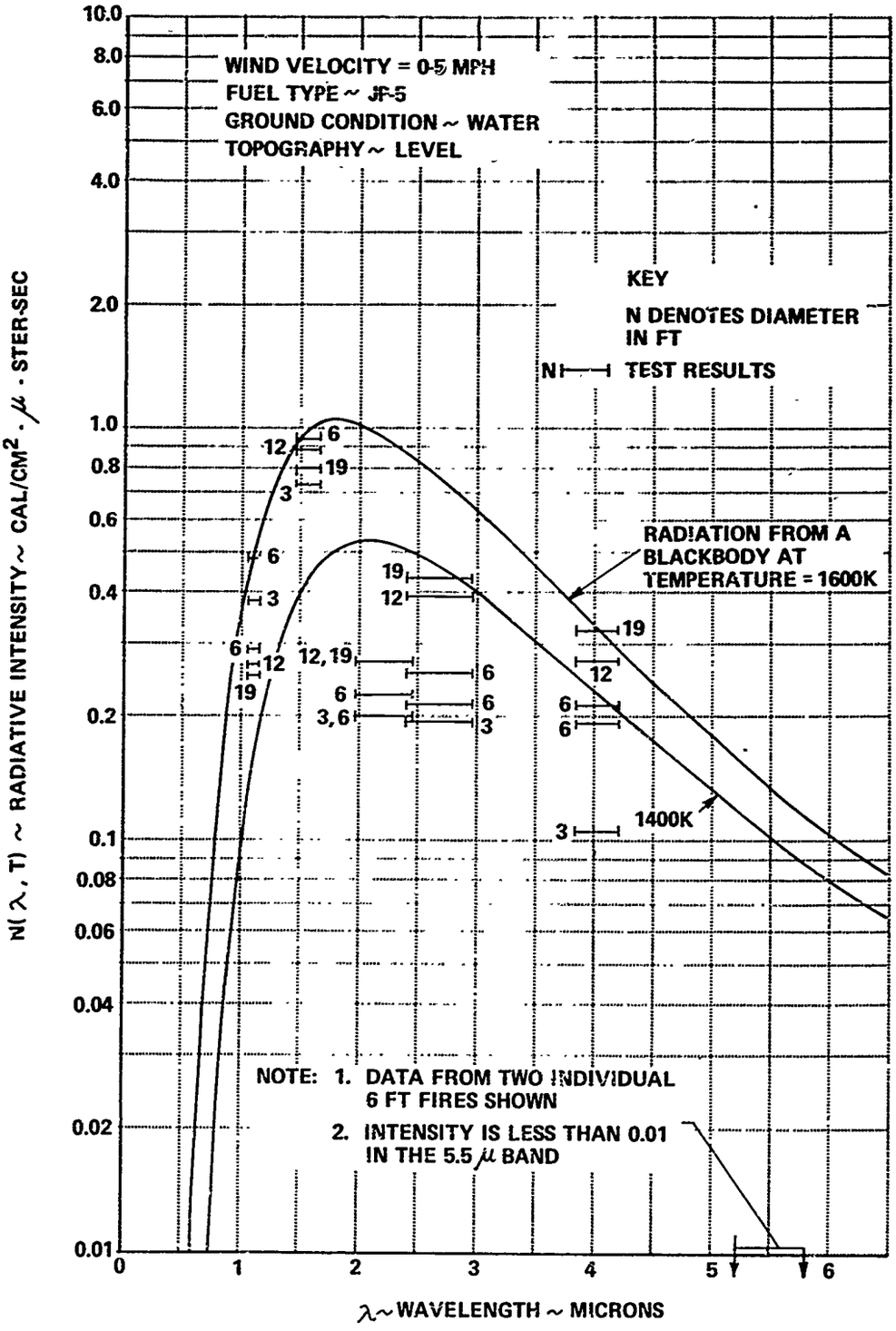

Figure 11 EFFECT OF POOL SIZE (DIAMETER) UPON SPECTRAL INTENSITY OF FLAME RADIATION

Topography

During two fires the heat meters that were aligned with the wind were arranged so that their elevation increased with distance from the one farthest upwind (as in Figure 12). The meters placed in the line extending away at 90° to the wind were at the same elevation as with other tests. The maximum height (6 ft.) represents the maximum value of interest to personnel near the fire. In some respects, this arrangement is similar to a special situation on a hillside, whereby the wind is blowing in the uphill direction. In such a case the flames would flow closer to the ground than otherwise, and the plots in Figure 13 show this kind of effect. Here, data are plotted from fires No. 11 and 16 for comparison. The arrangement does not provide complete representation of the hillside situation because the correct boundary layer condition is not reproduced between the flowing air and the ground. Moreover, the boundary layer for wind flow over the ground is greatly dependent upon ground roughness and type of vegetation so that no single situation is typical of all hillsides. More work is needed on the effects of topography.

Most of the time during the fire (No. 16) the wind velocity and direction were of the required combination for the flames to blow along the row of downwind meters, rising along the line of meters at almost the same slope. This is reflected by the results of Figure 13, and it indicates the magnitude of downwind convection at 12 ft. away (the difference between the curves for meters level and sloping). No upwind data were available from fire No. 11 for a direct comparison of upwind heating rates. It is interesting to note that the peculiar distribution of heating in a direction 90° to the wind was also obtained for the two fires represented in Figure 13. It is significant to point out here that the data for each side curve were obtained from a different set of heat meters. The side heating data points at 12 ft. away for each fire display a large difference for two fires that were supposedly burned under the same conditions, and the only comment pertinent to this is that fires are transient phenomena.

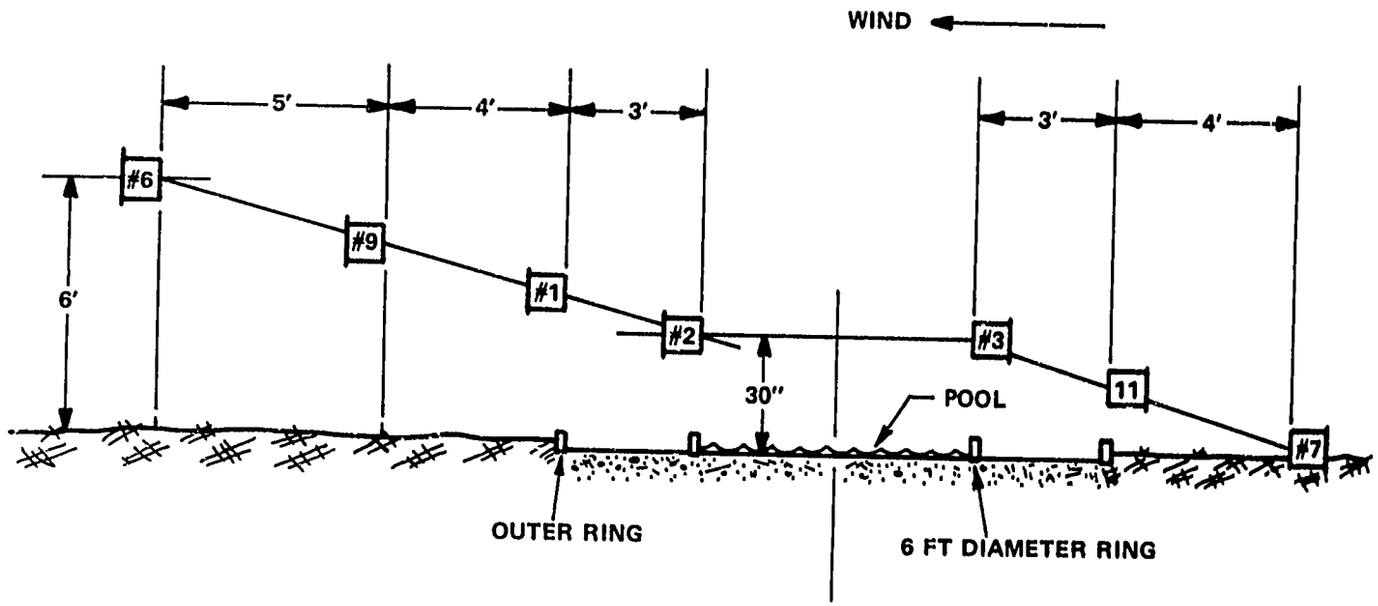

Figure 12 HEAT METER ELEVATIONS, FIRE NOS. 10 & 16

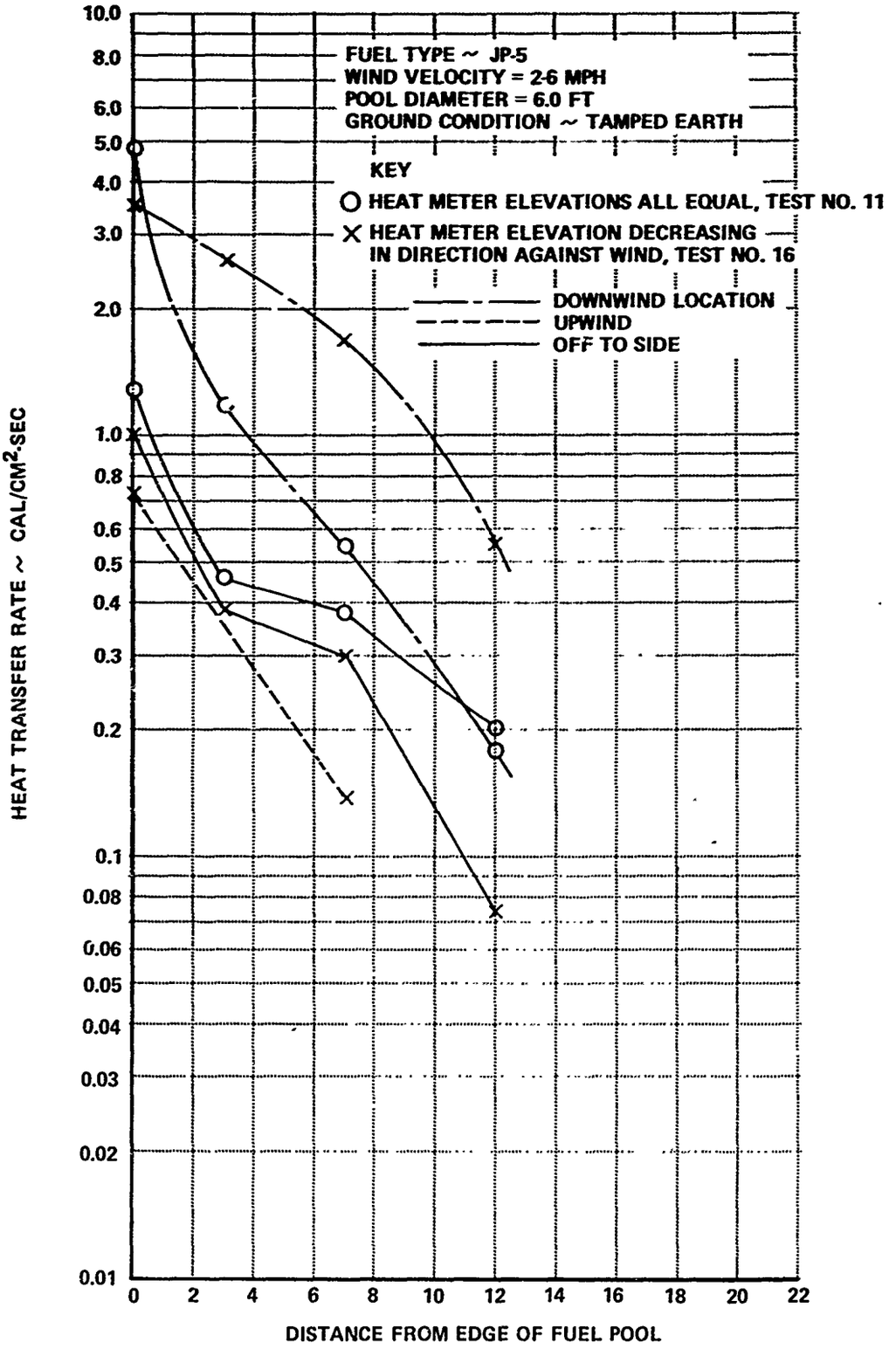

Figure 13 EFFECT OF ELEVATION UPON HEATING RATE TO A SURFACE NEAR FIRE FROM BURNING AIRCRAFT FUEL

Miscellaneous Objects

Figure 14 gives comparative heating distributions around burning JP-5 with and without a large object within the fire. In one fire, a 55-gallon drum with one end cut open was placed on its open end so that its centerline was displaced 15 in. away from the center of the pool in a direction towards the crosswind heat meters. Two obvious effects can be seen in Figure 14. First, the heat intensity at the crosswind meters is reduced by the presence of the drum. Second, the intensity along a downwind radius decreases more rapidly in the case of the fire with the drum. The fact that the drum was displaced towards the crosswind meters caused it to shade them from part of the fire, and this may be the major cause of the first effect. Additionally, however, the photographs, Figure 15, show that an enlarged area of flames occurred in the lee side of the drum, with a nearly level top extending beyond it for at least 6 ft. This was not a steady condition (some pictures showed a lower flame profile), but it may account for the peak levels of heating shown in Figure 14.

During the fire with the drum in it, the meter at the edge of the pool in the downwind location showed a much lower heat flux than did the meter at 3 ft. from the edge. This was a result of its location above the flames, which were quite low, whereas the other downwind meters were well aligned with the flames. Data from the radiometers were of no assistance in determining effects of miscellaneous objects. All that was shown was the decreased radiative intensity from shallow flames that were exposed to view at either side of the object. Upwind heating was greatly reduced by the object.

Fire Toxicity

Samples were obtained of the air near the edge of flames for several fires for the purpose of determining the extent of contamination caused by fire. The location of each sampling station is shown in the plan of Figure 16. Figure 17 shows the contaminant distribution along a vertical, directly downwind, and below the flames (station 6). Figure 18 shows a horizontal distribution downwind but closer to the pool and off to one side of the fire (outboard

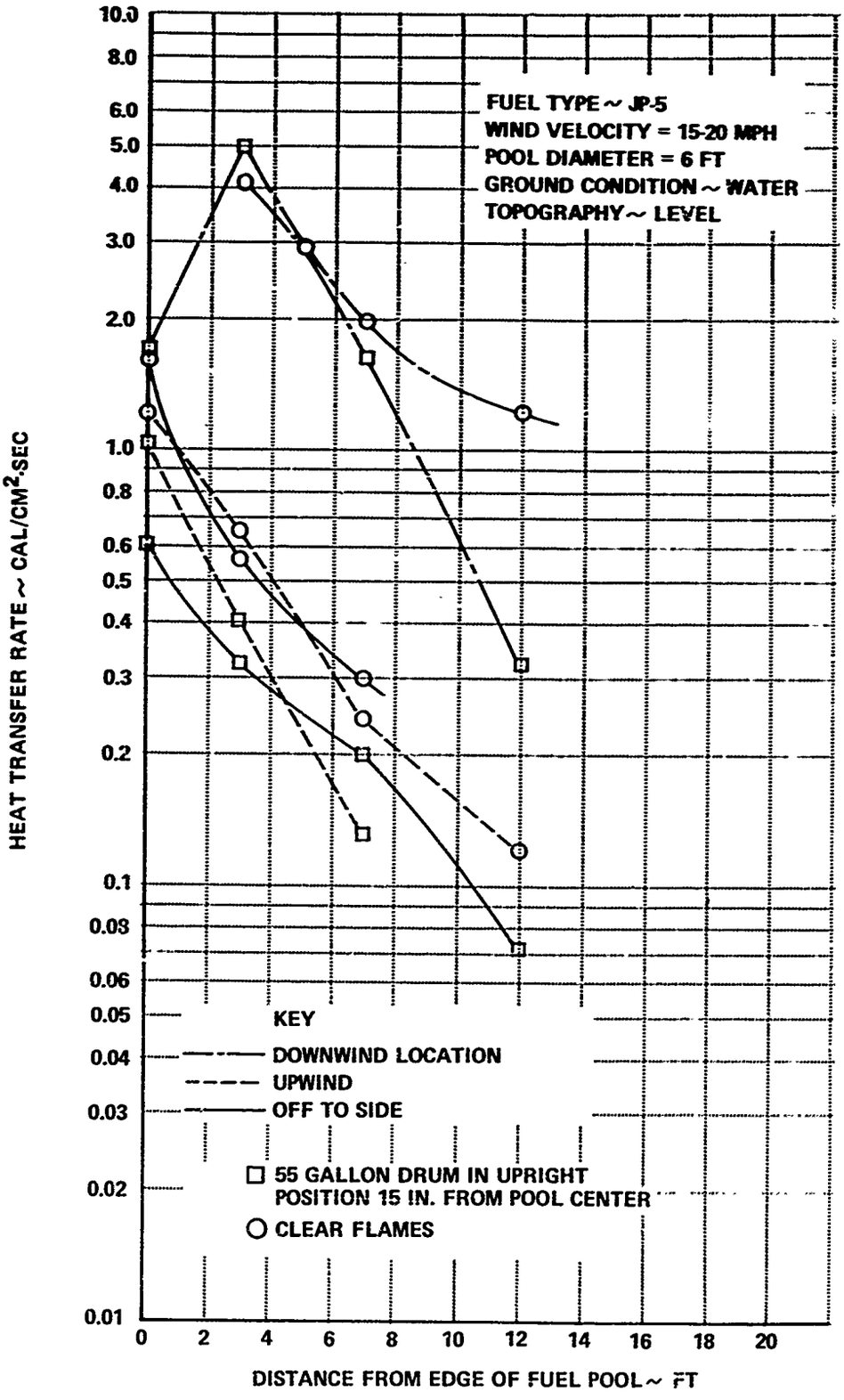

Figure 14 EFFECT OF OBJECT IN FIRE UPON HEATING RATE TO A SURFACE NEAR FIRE FROM BURNING AIRCRAFT FUEL

Figure 15 FIRE WITH EXTRANEOUS OBJECT

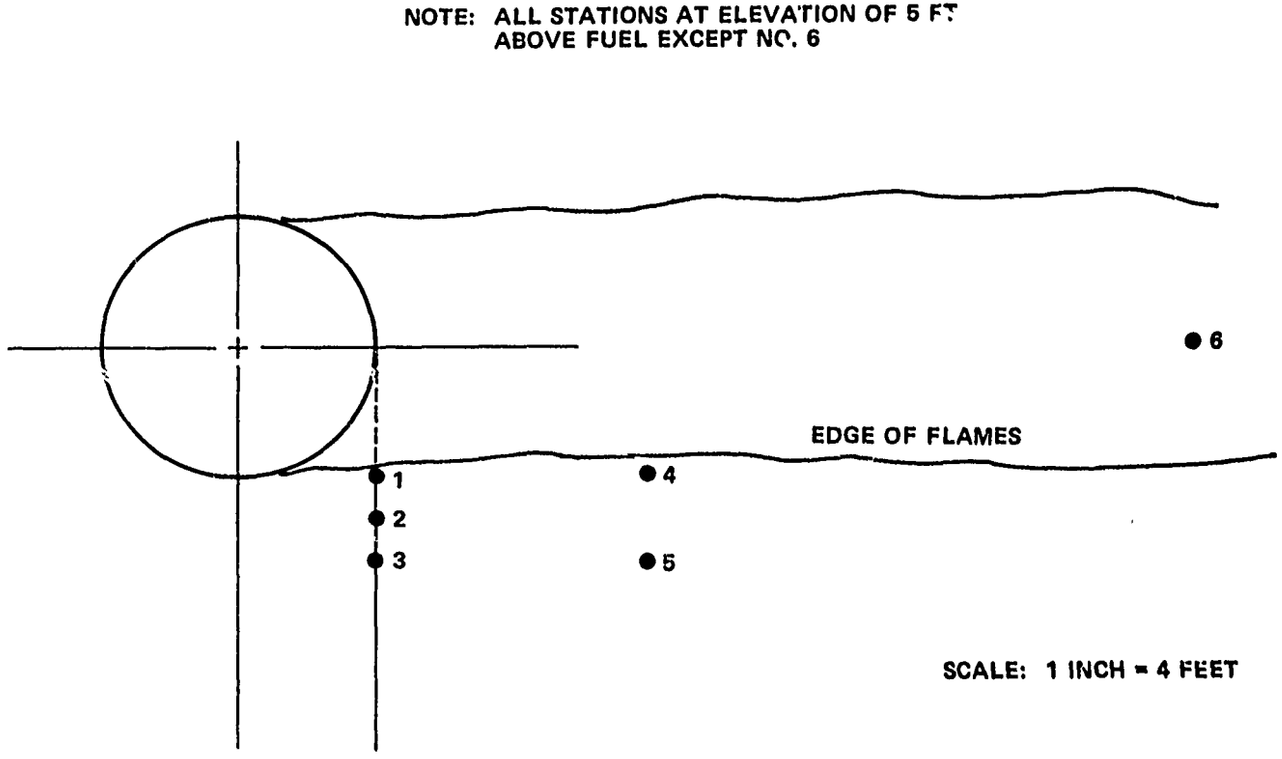

Figure 16 LOCATION OF GAS SAMPLING STATIONS

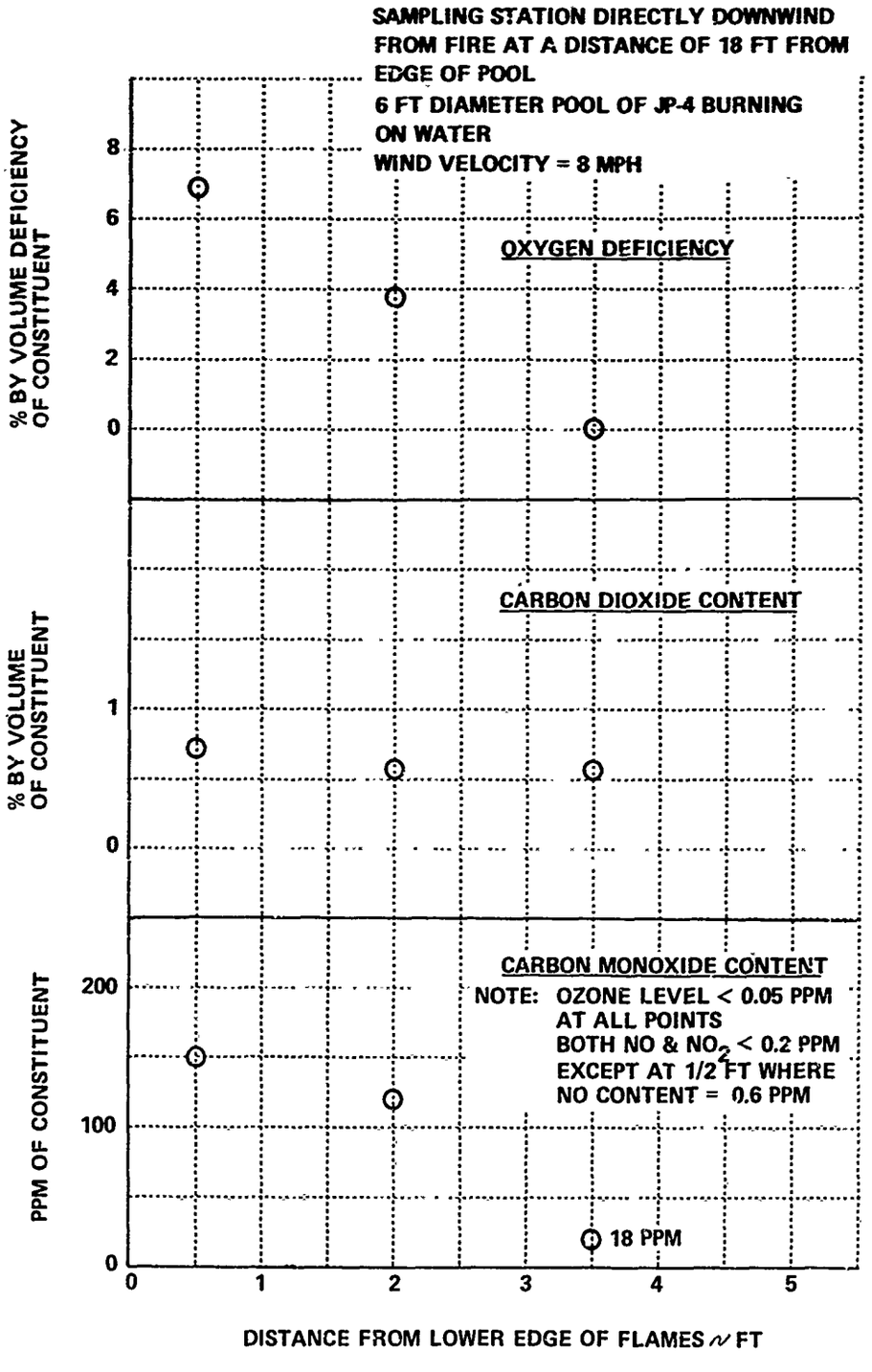

Figure 17 VERTICAL AIR CONTAMINANT PROFILES

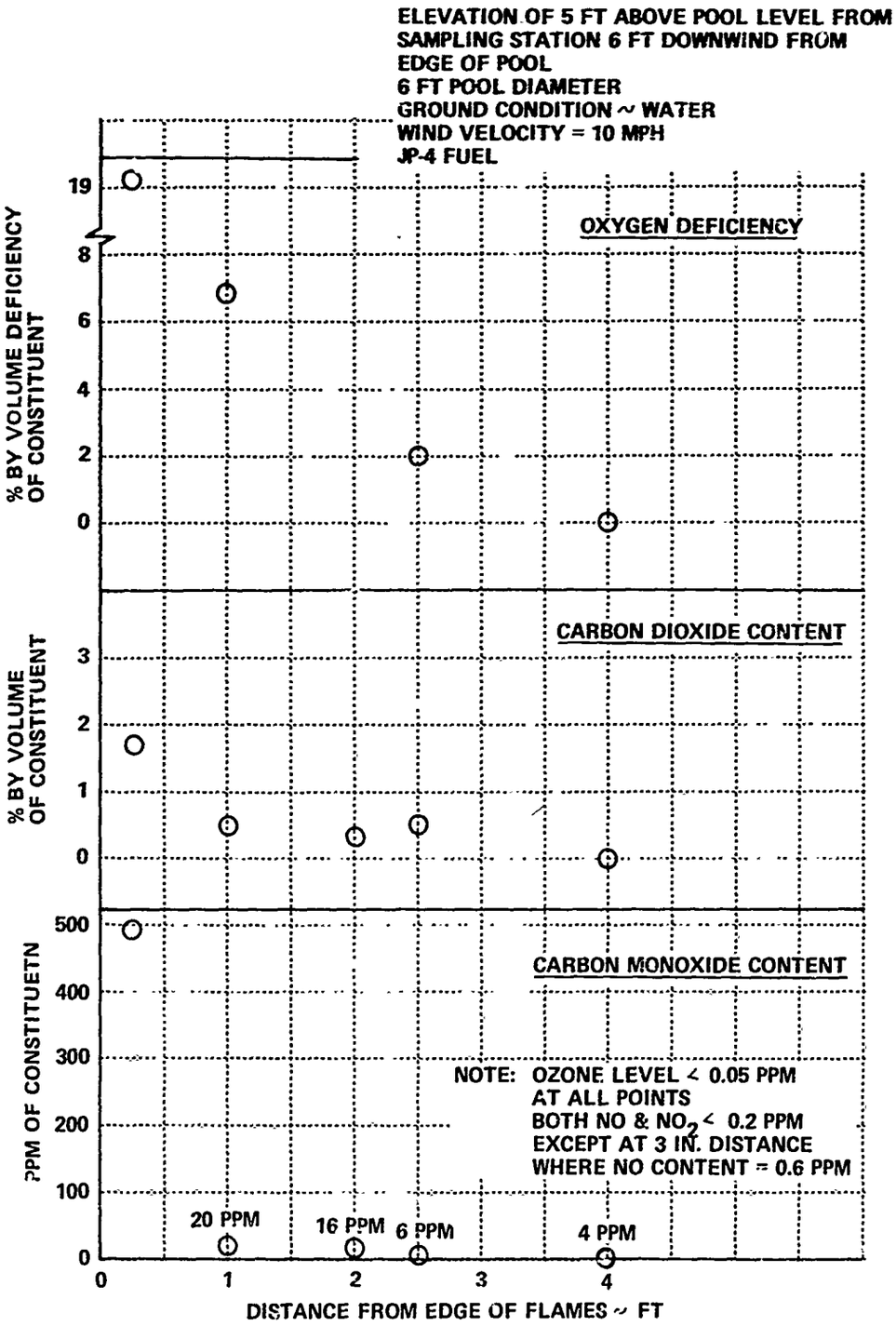

Figure 18 HORIZONTAL AIR CONTAMINANT PROFILES

from station 4). The minimum values given by the notes represent the minimum detection capability of the detector and otherwise signify that the analysis yielded no indication of the presence of the gas in question. Additional data for JP-4 fires are presented in Table IV. Data for a JP-5 fire are given by Table V.

General Discussion

The radiometer data reveal some interesting effects, in addition to those already discussed, relative to total heating rates. First, note that curves for the theoretical spectral distribution of blackbody radiation are plotted for two temperatures (of the blackbody). Each curve represents the maximum possible intensity that may be radiated from any object or gas cloud at the specified temperature and at each wavelength. Consequently, it may be stated that 1600°K is the minimum flame temperature that can account for the experimental results depicted. For example, Figure 5 shows that the blackbody curve falls upon the maximum measured values of flame radiation at 1.1 and 1.55 micron wavelength. If the flames (or their suspended soot particles) emit radiation as effectively as a blackbody, their temperature must have been 1600°K. If not, it means that their temperature was higher than this. It is known that suspended soot particle clouds of moderate number density are effective emitters,(Ref. 1), at least at the short wavelengths. However, at 2.2 microns, Figure 5 shows that the emission of flames was poor even for the large fires. If 1600°K is presumed to be the emission temperature of the flames, the spectral emittance at 2.2 microns can be computed using the blackbody intensity of 0.93 cal/cm^2-μ-ster.-sec. The measured intensity is 0.27 for the larger fires, so the emittance is 0.27/0.93 or $\epsilon_\lambda = .29$. Note that this band is just beyond the nearest atmospheric absorption band for H_2O (2.5 to 2.7μ, Ref. 2 and 3) so that atmospheric absorption does not account for the reduced intensity. However, absorption by the atmosphere could be the explanation for the lack of response demonstrated by No. 6 radiometer in the 5.2 to 5.8 micron band. It is shown by Ref. 2 that H_2O absorption accounts for more than 1/3 of the emitted radiation over a path length of

TABLE IV

AIR CONTAMINATION NEAR JP-4 FIRE

(Burning on Water in a Pool of 6 ft. Diameter)

Sampling Station No.	Gas	Concentration
1	CO	No Indication
(Wind velocity = 10 mph)	CO_2	0.17 percent by volume
2	CO	4 ppm
(Wind velocity = 10 mph)	CO_2	0.39 percent by volume
3	CO	12 ppm
(Wind velocity = 8 mph)	CO_2	0.21 percent by volume

NOTE: Ozone level was <0.05 ppm for all fires . NO and NO_2 level both <0.2 ppm for all fires. No hydrocarbons detected. No tests made for oxygen deficiency.

TABLE V

AIR CONTAMINATION NEAR JP-5 FIRE

(Burning on Water in a Pool of 6 ft. Diameter)
(Wind Velocities = 11 mph)

Sampling Station No.	Gas	Concentration
1	CO	12.3 ppm
	CO_2	0.37 percent by volume
	NO_2	<0.2 ppm
	O_2 deficiency	0
2	CO	24.6 ppm
	CO_2	0.57 percent by volume
	NO_2	<0.2 ppm
	O_2 deficiency	0
4	CO	900 ppm
	CO_2	2.9 percent by volume
	NO_2	4.9 ppm
	O_2 deficiency	4.0 percent by volume

NOTE: Ozone level was <0.05 ppm for all three samples. NO_2 level was <0.2 ppm for all three samples. No hydrocarbons detected.

50 ft. (1520 cm) between 5.2 and 5.8 microns, wavelength, at a vapor partial pressure of 9mm of mercury (corresponding to 70 percent relative humidity at 60°F).

The emittance of aviation fuel flames is shown to be high at the 1.1 and 1.55 micron bands. It is low for the 2.2 and 2.7 micron bands, but at these wavelengths the emittance is increased by the size (depth) of the fire. This is also the case at 4.0 microns, where emittance appears to be at or near a maximum for the 19 ft. fire (18 2/3 ft. actual diameter) because its radiant intensity falls upon the 1600°K blackbody curve.

Comparisons with spectral radiation data obtained by other researchers could not be made directly because of differences in either their experimental conditions or type of fuel. Ref. 4 shows results for benzene flames of small dimensions although effects of increasing ambient pressure are shown, and it can be appreciated that increased pressure causes increased intensity at all wavelengths just as increased flame depth does, below certain limits. However, this was not pool burning. The continuum spectrum for flames from a pool of benzene is given by Ref. 5, which is more significant. A comparison reveals that intensity of radiation from the benzene flames falls off at a higher wavelength, i.e., 2.5 microns instead of the 2.0 microns obtained for the aircraft fuel fires. Also, intensity is higher at 3.0 microns for the benzene flames than for the larger aircraft fuel fires.

A very peculiar effect was shown for all the spectral plots of Ref. 5 that was not explained satisfactorily--this is the high intensity peak at 4.5 microns. An actual intensity of such magnitude could only be produced by flames of extremely high temperature, exceeding 3000°K. If this were the case, the emissivity at other wavelengths would have to be very low in order to produce the results shown by Ref. 5. It can only be concluded that the data of Ref. 5 at 4.5 microns is meaningless.

V . SIGNIFICANCE OF FIRE CHARACTERISTICS TO THE DESIGN OF PROTECTIVE CLOTHING

The two thermal properties of protective clothing that most affect its response to incident heating, such as that imposed in the vicinity of a fire during long time exposure, are the surface reflectivity and the thermal conductivity of each layer of material composing the clothing. For brief exposure to intense heat the specific heat and the density of the insulating layers will also be important.

If the rate of heating (heat flux) absorbed by a garment is known, and if this rate is assumed to be steady, i.e., constant, the rate at which heat is transmitted through a garment of a defined thickness may be computed from the above-mentioned thermal properties; or, vice versa, the property requirements and/or thickness can be computed from a specified rate of heat transmitted. At the surface an energy balance prevails, and it may be expressed as $q_s = q_{ir} + q_c - q_{rr} - q_{ref}$, which states that at any instant, the heat absorbed at the surface, q_s, equals the incident radiative energy plus the convective heating (or minus the convective cooling, as the case may be), minus the heat reradiated by the surface to space, q_{rr}, minus the energy reflected, q_{ref}. The convective heating, q_c, may be ignored for garments to be designed for use outside the flame zone, because convective heating does not extend much beyond the flame zone down near the base, except for positions directly downwind. Therefore, protection against convective heating is of less consequence to this program than protection against radiation.

The reradiated energy from the clothing is also expected to be negligible relative to the net absorbed radiation at locations near the fire edge due to the relatively low temperature of the clothing compared to the fire. The reflected energy, q_{ref}, is ρq_{ir}, where ρ is the total hemispherical reflectivity. Hence, to a good approximation near the fire edge, $q_s = q_{ir}(1-\rho)$, where the reflectivity of the clothing, ρ, is a function of wavelength, λ.

The experimental data of this program allow determination of q_{ir} for fires at various conditions. The incident radiative heating may be expressed as $q_{ir} = F\int_0^\infty N d\lambda$, where F is a form or shape factor determined by the geometry of the interchange and the emittance values for source and receiver. See Ref. 4 for typical values of F. The integral $\int_0^\infty N d\lambda$ is identical to σT^4 for a blackbody but for fires must be determined from the measured spectral distributions of radiation. Figure 19 illustrates these distributions for JP-5 fuel. Figure 20 illustrates the integral $\int_0^\infty N d\lambda$ for two pool sizes. In addition, plots are given for blackbody distribution at 1600°K, the best estimate of flame temperature.

The value of the total normal radiative intensity, $\int_0^\infty N d\lambda = 1.77$ cal/cm^2-ster.-sec., is indicated by the end value of $\int N(\lambda, T) d\lambda$ at $\lambda = 6$ microns. It follows that the maximum radiative intensity that would be sensed from a fire of infinite area and depth is $\pi\int_0^\infty N d\lambda$ or 5.56 cal/cm^2-sec. (1.77π). It can be determined that the radiative intensity sensed near a fire extending to infinity in directions both skyward and laterally along a ground plane would be half the maximum intensity or 2.78 cal/cm^2-sec. in this case. Of course, actual realization of this would require a uniform flame temperature of 1600°K throughout the fire.

To establish the actual radiation incident upon a firefighter from fires of wide extent, use must be made of the experimental heat meter data rather than the radiometer data because the heat meters measure the overall effect of the fire which exhibits finite flame height and temperature gradients throughout the flame. Attempts have been made to fit the heat meter data to the simple inverse square form, $q_{ir} = K A_o / X^2$, but these have met with poor success except at a distance from the fires exceeding 10 ft. However, most of the upwind heat meter data, and some of that obtained from the side meters, may be represented by exponential functions, as demonstrated by their straight line behavior on a semi-log plot (Figure 21). Some of these data have been replotted in Figure 21 as form factors, $F = q/\int_0^\infty N d\lambda$, versus distance from the center of the pool rather than the edge of it. It appears from Figure 21 that F = 0.20 is an upper limit for radiation from the experimental JP-5 fires.

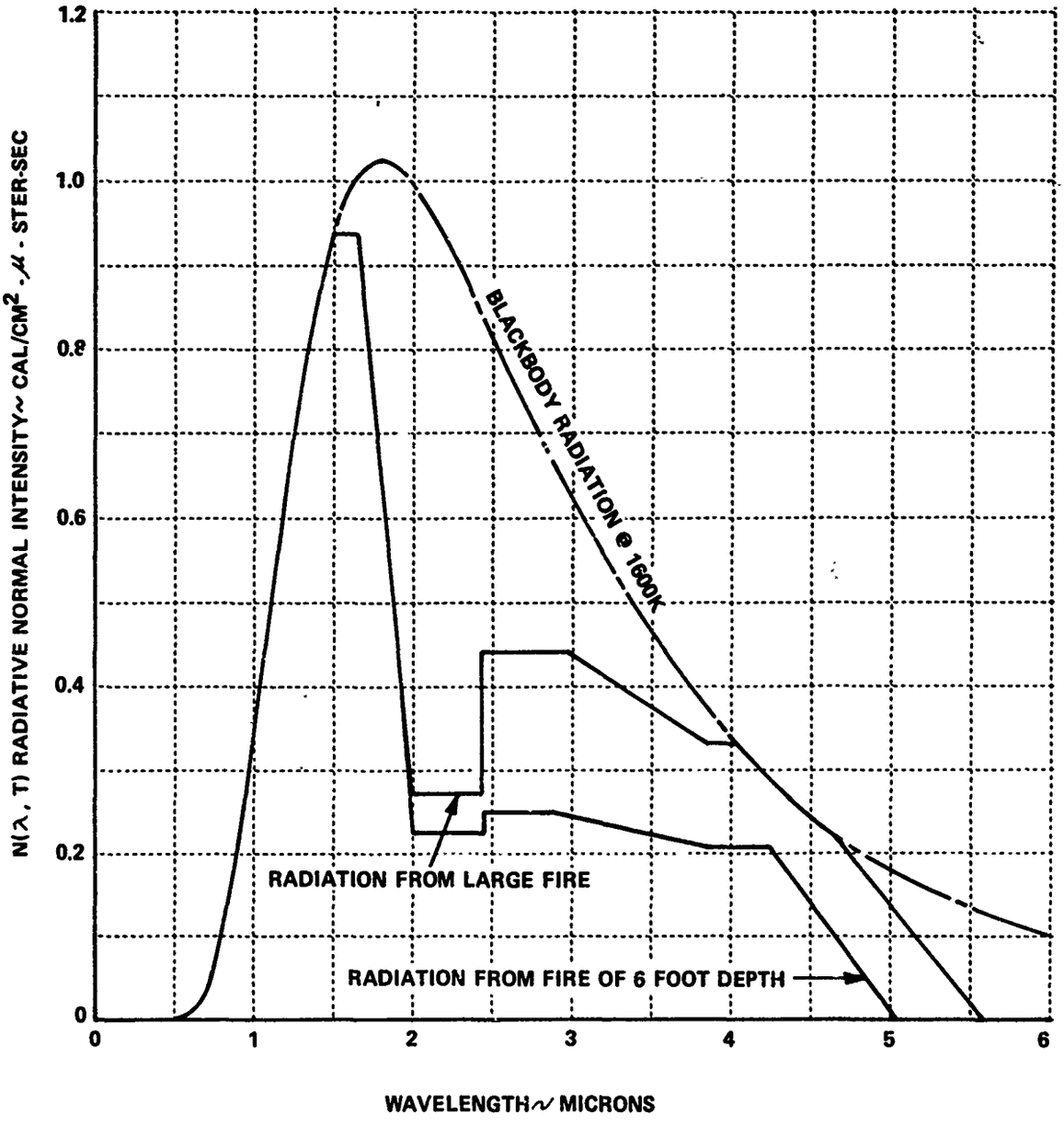

Figure 19 SPECTRAL INTENSITY OF FLAME RADIATION USED TO OBTAIN SUMMATION, $\int N(\lambda, T)d\lambda$

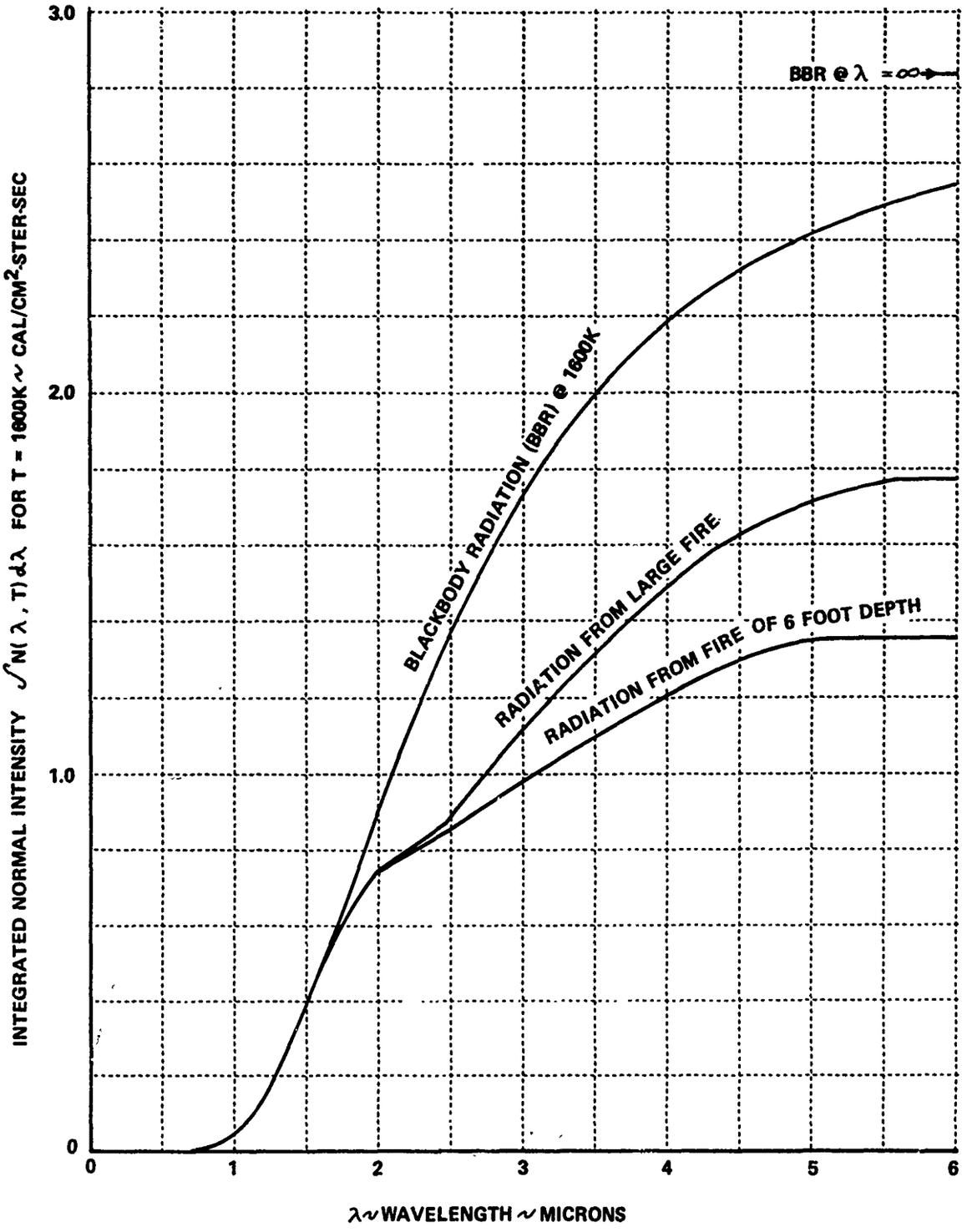

Figure 20 SUMMATION OF RADIATION OVER INFRARED SPECTRUM

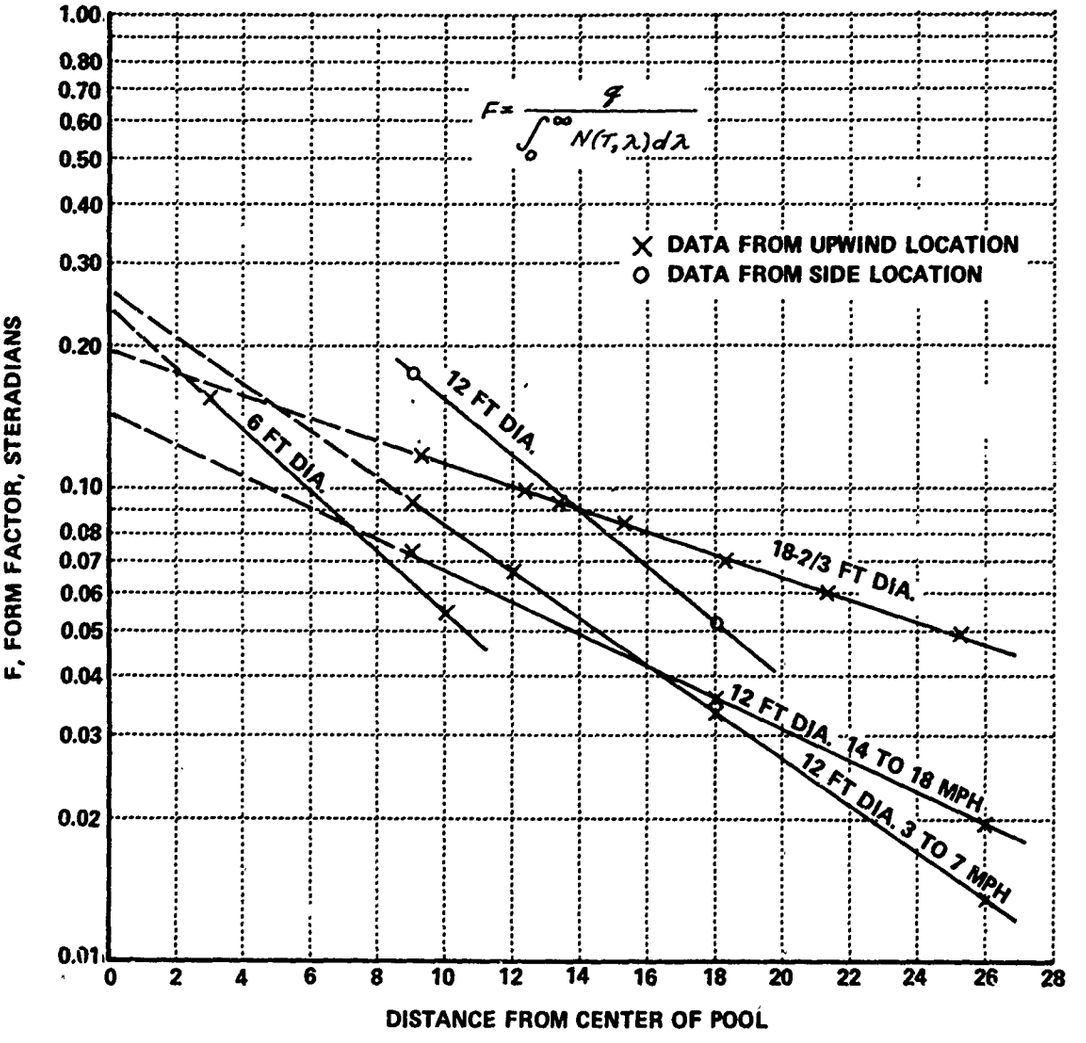

Figure 21 FORM FACTORS FOR JP-5 FIRES

To extrapolate this result to larger fires a few more observations must be invoked. First, the experimental fires were of finite depth, and the largest one exhibited peak radiative intensity from flame regions near its center as demonstrated by the radiometers, which showed that the intensity from the center of an 18 ft. fire was not much more than from a 12 ft. fire. However, regions near its extremities did not radiate at maximum intensity because of diminished flame depth and, possibly, reduced flame temperature. Now the heat meters sense overall radiation and are not limited to radiation from a small portion of the fire, and this fact must be considered in evaluating the form factor. The significance of flame depth will be determined by calculating the minimum flame depth that exhibits the same emissivity as very deep flames. This will permit an evaluation of the view angle that includes path lengths greater than the minimum path length. Also, it is well known that suspended soot particles are responsible for most of the energy radiated from hydrocarbon flames, Ref. 1. The nature of this emission has been formulated as total emissivity in terms of path length, L, through the radiating medium, Ref. 6;

$$\epsilon \simeq 1 - 1/(1 + KT f_v L/C_2)^4$$

where f_v is the soot concentration per unit volume, and C_2 is a constant. A similar expression was developed in Ref. 7. Now a ratio of the $\int_0^\infty N d\lambda$ for the fire and a blackbody at the same temperature yields total emissivity. Using the results of Figure 20, it is determined that $\epsilon = 0.47$ for the 6 ft. fire (path length = 4 ft., as scaled from the photographs) and $\epsilon = 0.625$ for the large fire (maximum L = 12.7 ft.). Fitting the data for the 6 ft. fire to the relation for emissivity above, a value for KTf_v/C_2 of 0.043 ft.$^{-1}$ is obtained. Then this is applied to the determination of the value of L for which the maximum flame emissivity is reached (as represented by $\epsilon = 0.625$ for the large fire), and it is found that L = 6.5 ft.; i.e., any fire thicker than 6.5 ft. is expected to have an emissivity of 0.625. Next, it can be determined for the geometry of the fire in a horizontal plane that $L = 2r \cos\theta$ when X = 0, i.e., for the

target at the edge of the flames (see sketch below). The circle represents

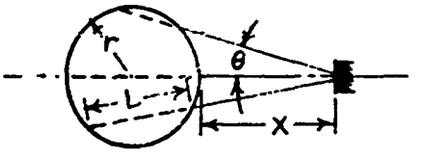

the extremities of flames and the dashed portion of each of the rays represents flame depth or path length for radiation along the ray. For the largest experimental fire, the 6.5 ft. value of L is obtained for $\theta = 59°$. Beyond this angle, path length falls very rapidly and with it emissivity. Therefore, the radiative energy emitted by flames outside the plane described by this angle may be neglected. Using this result, an extrapolation of F may be made for flames of infinite extent and the same height as the experimental fire on the 18 2/3 ft. pool. Specifically, if $F = 2.0$ for $\theta = 59°$, then $F = 90/59\ (0.2) = 0.3$ for $\theta = 90°$. Because $F = 0.2$ corresponds to an optically opaque fire within view of an included angle of 118°, the value $F = 0.3$ is appropriate for a fire extending to infinity in opposite directions, i.e., for an included angle of 180°. A negligible increase in F is obtained by a similar treatment of the fire in a vertical projection even though the fire is of finite height. An additional increment in F would be calculated for JP-4 (and probably an equal one for gasoline) fires because of a radiative intensity 15 percent higher than for JP-5 (see Figure 2c).

Therefore, it can be concluded that the maximum radiative heating emitted from liquid fuel fires and incident upon a vertical surface near the ground is $0.3\ (1.15)\ 5.56 = 1.9$ cal/cm^2-sec. In addition, the form factor for targets at various distances from a fire of finite height (about 30 ft.) and depth (about 18 ft.), but infinite width was estimated from a projection of the geometry in a vertical plane normal to the edge of the flames, based upon the measured data from the 18 ft. diameter experimental fire. (The 30 ft. height was estimated by observation of the fire because the photographs did not encompass the complete view). The results of this estimate are plotted in Figure 22 as radiative heating rate vs. distance from the flames. It is recommended that the design condition for heating rate be selected from this curve if it is to be dictated by the proximity to the fire that the firefighter must assume.

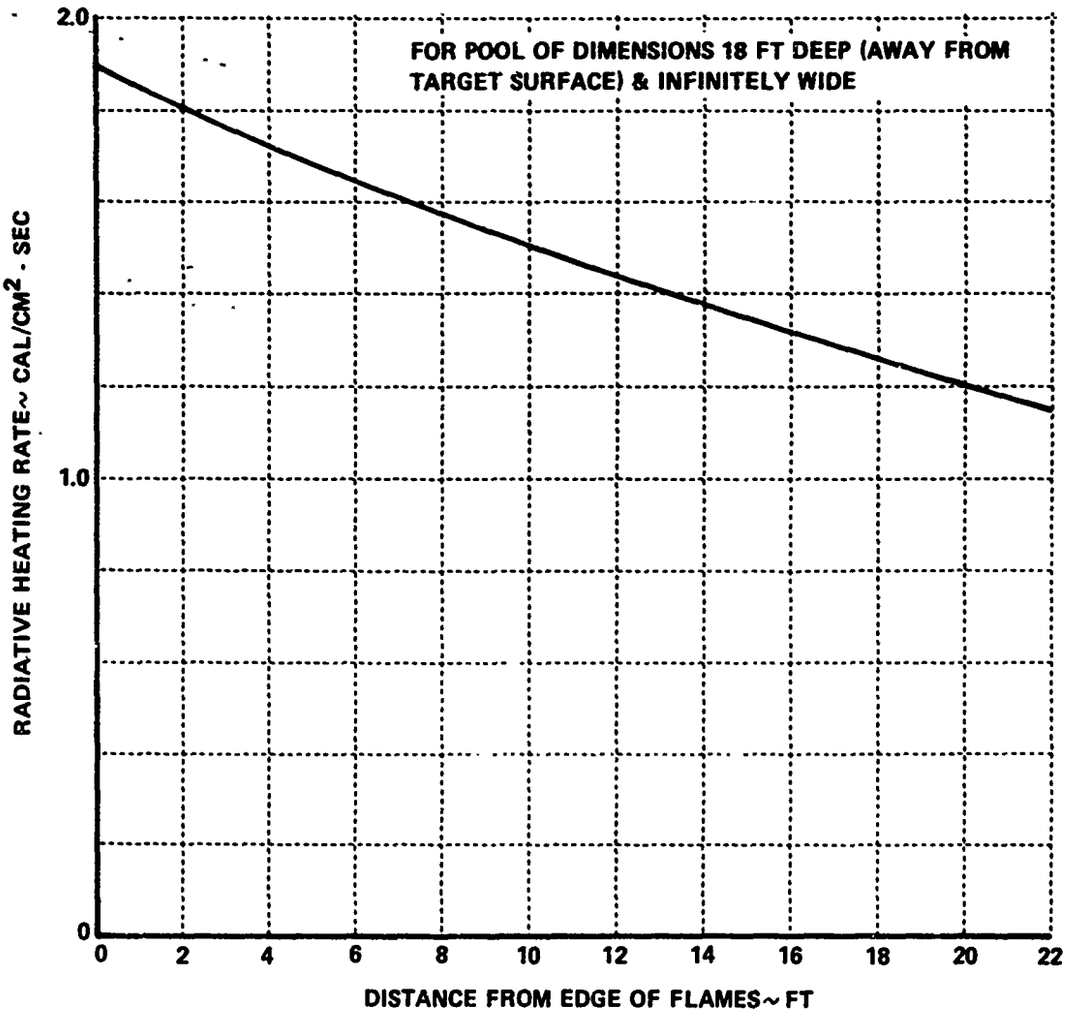

Figure 22 MAXIMUM RADIATIVE HEAT TRANSFER RATE TO SURFACES IN VICINITY OF BURNING POOL OF JP-4

It is obvious that most of the intense heat encountered near flames may be rejected by employing protective surfaces with high reflectivity. Because of the variation of the radiative intensity over the spectrum, e.g., Figure 19 a second consideration is that high reflectivity is most important in the bands of high emission. The particular band or wavelength is important also, because the maximum possible intensity varies with wavelength.

To aid in the selection of surface material, a chart (Figure 23) has been prepared for determining the rate of heat absorbed at the surface that is based upon the spectral distribution of the large fire, as depicted by the solid lines of Figure 19, and a maximum output of 1.9 cal/cm^2-sec. The chart is intended to be used with plots for distribution of reflectivity such as shown by Figures 11.8 and 11.9 of Ref. 8. It is necessary to choose an average value of the monochromatic reflectivity for the band indicated for each subplot of the chart. Then each subplot may be entered with its value of reflectivity to determine the increment of heating contributed by its radiation band. The total of the increments for all six subplots yields the heat absorbed by a vertical surface at the edge of the flames. The lower this total the better the material is in terms of thermal protection of the firefighter. To determine the heat absorbed at a given distance from the flames, read the radiative heating at that distance on the curve of Figure 22 and multiply the total obtained from the chart by the factor equal to radiative heating at a distance divided by 1.9.

As an example of a poor application of reflective material, a summation was made for good reflectivity, $\rho = 1.0$, in the 1.0 to 2.0 micron band and $\rho = 0.1$ throughout the rest of the spectrum. The distribution of absorbed energy is plotted as the dashed line of Figure 24, labeled No. 2. In spite of the high reflectivity up to 2.0 microns, much energy is absorbed (0.76 cal/cm^2-ster.-sec.). A better example is given for $\rho = 0.1$ up to 1.65 microns and $\rho = 1.0$ beyond. The result is plotted as a dashed line labeled 1, and the absorbed energy at the surface is 0.49 cal/cm^2-ster.-sec.

DIRECTIONS: SELECT AVERAGE REFLECTIVITY OF SURFACE FOR EACH RANGE OF WAVELENGTH (BAND) INDICATED FOR THE VARIOUS SUBPLOTS SHOWN. USE EACH SUBPLOT TO FIND THE CORRESPONDING INCREMENT OF HEATING RATE. SUM THE INCREMENTS TO FIND THE TOTAL

EXAMPLE: ALUMINIZED PAINT
ρ FROM REF 8

$\lambda \sim \mu$	ρ	Δq_s
0.63	0.73	0.055
1.50	0.76	0.110
2.13	0.78	0.068
2.75	0.77	0.052
3.5	0.77	0.092
5.0	0.78	0.065
	q_s =	0.442

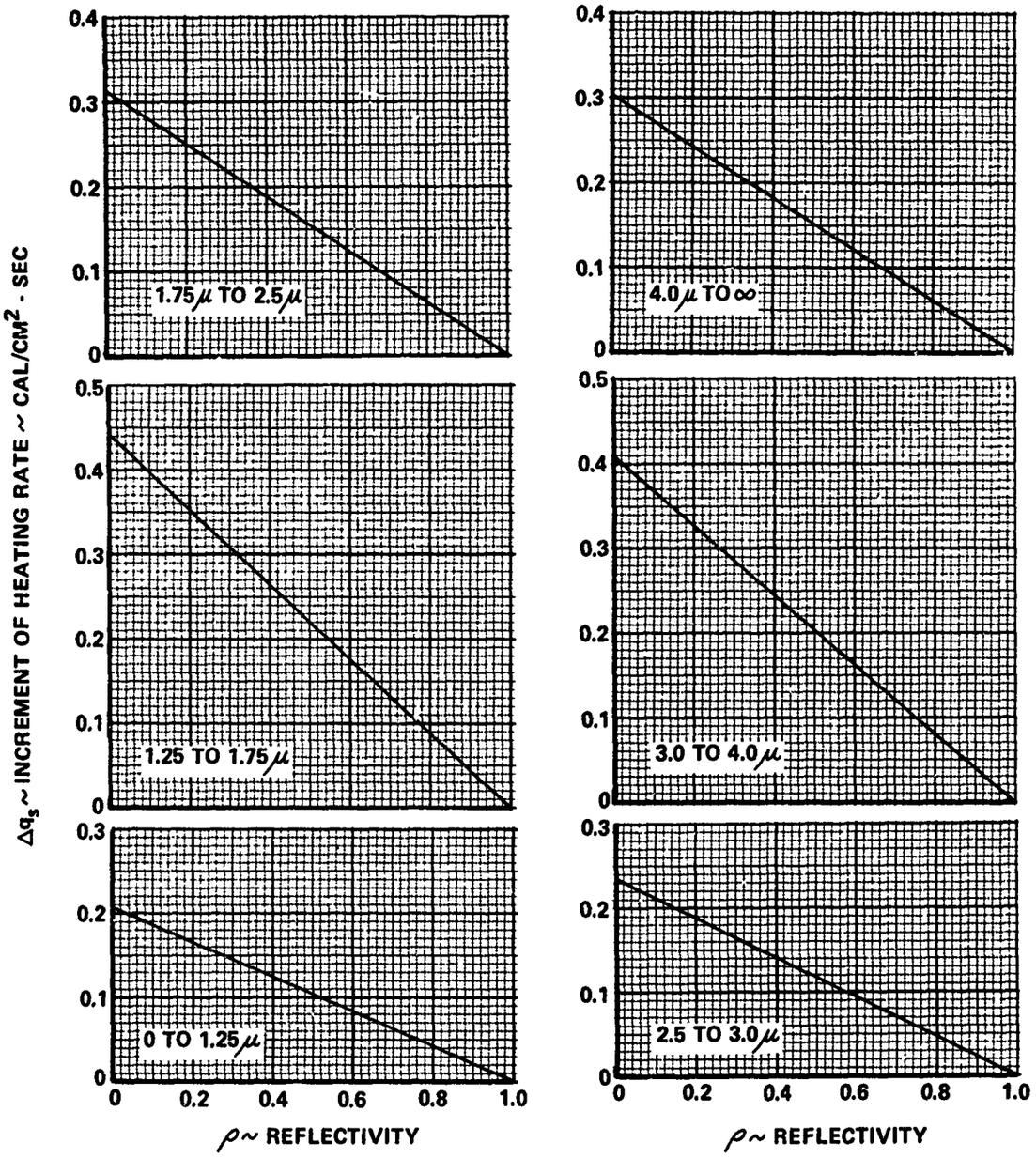

Figure 23 CHART FOR DETERMINING HEAT ABSORBED BY SURFACES EXPOSED TO LARGE AIRCRAFT FUEL FIRE

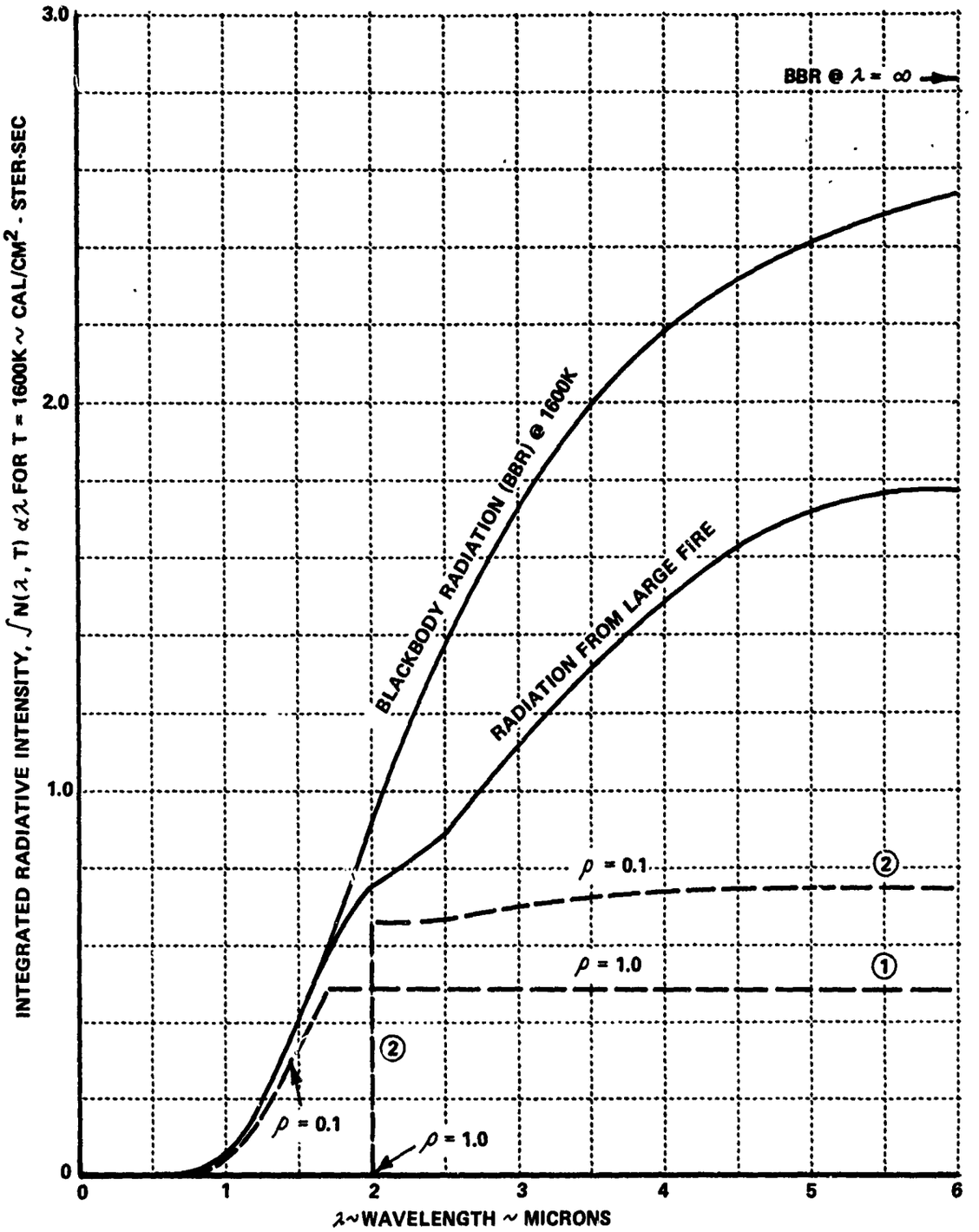

Figure 24 TOTAL RADIATIVE HEATING ABSORBED BY HYPOTHETICAL SURFACES

VI. CONCLUSIONS

The following conclusions may be drawn as a result of the experimental measurements:

1. The chief effect of changing wind velocity upon radiative intensity sensed near fires was to change the geometry of the flame-target interchange. There was no perceptible change in normal spectral intensity as indicated by radiometers, so estimates of infrared radiation from extremely large fires are not influenced by effects of wind velocity.

2. Increased wind velocity caused increased convection heating at a given distance downstream from the fires for a fixed elevation. Convection effects at other orientations to the fires relative to wind direction were negligible beyond 3 ft. away from the flames and of minor effect at points 30 in. directly above the edge of the fuel pool.

3. Fuel burning on either bare concrete or water yielded higher total heating rates at the heat meters than fuel on earth, and increased radiative intensity was detected by the radiometers for fuel burning on water.

4. Avgas and JP-4 fires yielded 15 percent higher heating rate at the heat meters than did burning JP-5, although increased radiative intensity was not detected by the radiometers.

5. Radiative intensity in each radiometer band was either the same or only slightly higher for the fire on the 18 2/3 ft. diameter pool (for which flame depth was about 13 ft.) compared to the fire on the 12 ft. diameter pool, which indicates that increased pool diameter would have yielded only marginal increase in emission of radiative energy. In other words, the flame depth of 13 ft. is nearly the minimum required for maximum radiative emission from pool fires. This conclusion permits estimates to be made of radiative heating from larger fires, based only upon geometry defining the fire and target surface, and upon the experimental values of normal radiative intensity.

6. An object was placed in a fire that was of large surface area relative to pool burning area. The object served to redistribute the flames and shade a significant volume of the flames so that the radiative heating at the upwind heat meters was reduced considerably. The steel surface of the object was not sufficiently hot to add to the radiative heating incident upon the meters.

7. Flame temperatures for the fire, on pools of 6 ft. diameter or more, of 1600°K appear to be a reasonable maximum, as indicated by the radiometer measurements. The highest thermocouple reading was 1380°K or 2020°F. The difference between the two kinds of measurement is reasonable and can be attributed to thermocouple heat losses.

8. The effect of obstacles or terrain features that shield a firefighter from the flames may be estimated on a geometrical basis using the heating rate data obtained from the experimental fires.

9. The presence of toxic gases follows a pattern similar to convection effects, as anticipated. Dangerous levels were detected only very near or directly in the flames. It follows that if smoke and flames can be avoided, dangerous toxic gas levels will also be avoided.

10. The heat meters and radiometers that were selected for the experiments proved to be very well suited to the purpose. They were sufficiently responsive, they facilitated data gathering, and were relatively easy to calibrate. Furthermore, little or no degradation occurred with use, and this was especially important for the heat meters, which were repeatedly enveloped by flames.

11. It is believed that a sufficient characterization has been made of the extreme conditions of heating and spectral distribution of radiative energy near fires to permit an effective design of protective clothing for firefighters.

REFERENCES

1. Millikan, R. C., "Optical Properties of Soot," J. Optical Society of America Vol. 51, p. 278, 1961.

2. Burch, et al., "Infrared Absorption by Carbon Dioxide, Water Vapor and Minor Atmospheric Constituents," Air Force Cambridge Research Labs, Report No. AFCRL-62-698, July 1962.

3. Tourin, R. H., "Monochromatic Radiation Pyrometry of Hot Gases, Plasmas, and Detonations," Temperature, Its Measurement and Control in Science and Industry, Vol. III, Part 2, Reinhold Publishing Corp., 1962.

4. Eckert. E. R. G., and Drake, R. M., Heat and Mass Transfer, McGraw-Hill Book Company, Inc., 1959.

5. Kahrs, J., "Field Calorimetry/Chemical Studies (U)," Thiokol Chemical Corporation, Reaction Motors Division Report No. 5802-F to Edgewood Arsenal, Figure 5 (U), December 1965 (Confidential).

6. Baumeister and Marks, Standard Handbook for Mechanical Engineers, pp. 4-118, Seventh Ed., 1967.

7. Thring, M. W., Foster, P. J., et al., "Prediction of the Emissivity of Hydrocarbon Flames," Paper No. 96 of the proceedings of the 1961-62 Heat Transfer Conference at University of Colorado, Boulder.

8. Chapman, A. J., Heat Transfer, Second Ed., The MacMillan Company, New York, 1967.

9. Spencer, D. E., "Out-of-Focus Photometry," J. Optical Society of America," Vol. 55, No. 4, April 1965.

10. Gardon, Robert, "A Transducer for the Measurement of Heat-Flow Rate," Transactions of the ASME Journal of Heat Transfer, November 1960.

11. Communication to K. W. Graves by Mr. Donald Owens, Soil Technologist, of Cornell University, for the Erie Country Soil and Water Conservation District Office.

APPENDIX
EXPERIMENTAL APPARATUS

Radiometers

The radiometers used during the fire tests were designed specifically for this program. They were of the aperture or unfocussed type, which is simple and economical in addition to being well suited to the purpose, Ref. 9. Focussed radiometers were not deemed necessary for two reasons. First, refracting optics are both expensive and impractical for the broad range of infrared wavelengths covered. Second, reflecting optics are usually used at longer wavelengths, but this is necessitated only in case of weak signal levels and/or if a high degree of spatial resolution is required. However, the fires under consideration have the following characteristics: the source is of large extent, at relatively high temperature, and a very effective emitter. A high degree of spatial resolution is not required; rather, it should be avoided so that an averaging effect is obtained over a sizeable field of view. An advantage of unfocussed over focussed radiometers is that a known radiant quantity is measured, i.e., the average value of the source radiance over a known field of view (Ref. 9).

In relation to scanning spectroscopy, the advantage of unfocussed radiometry is that signals in each spectral band are continuous so that radiation from all wavelengths covered can be obtained simultaneously. Scan period for spectrometers was considered to be unduly long for application to fires. Thermocouple measurements have shown that temperature at a point within a fire varies rapidly over a wide range. This renders it impossible to complete a spectrum scan before a large temperature change occurs.

The aperture radiometer consists of a coaxial arrangement of two apertures separated by a fixed distance. A typical radiometer is shown in Figure A1. Six of these radiometers were fabricated from 1 in. I.D. heavy wall brass tubing, and all are basically the same except that the interference filters varied in thickness and diameter (up to 1 in. O.D. and 1/4 in. thick), and the detector housing for one was different so that it had to be clamped to the end of the tube instead of fitting inside. This was No. 6 (for the 5.5 μ

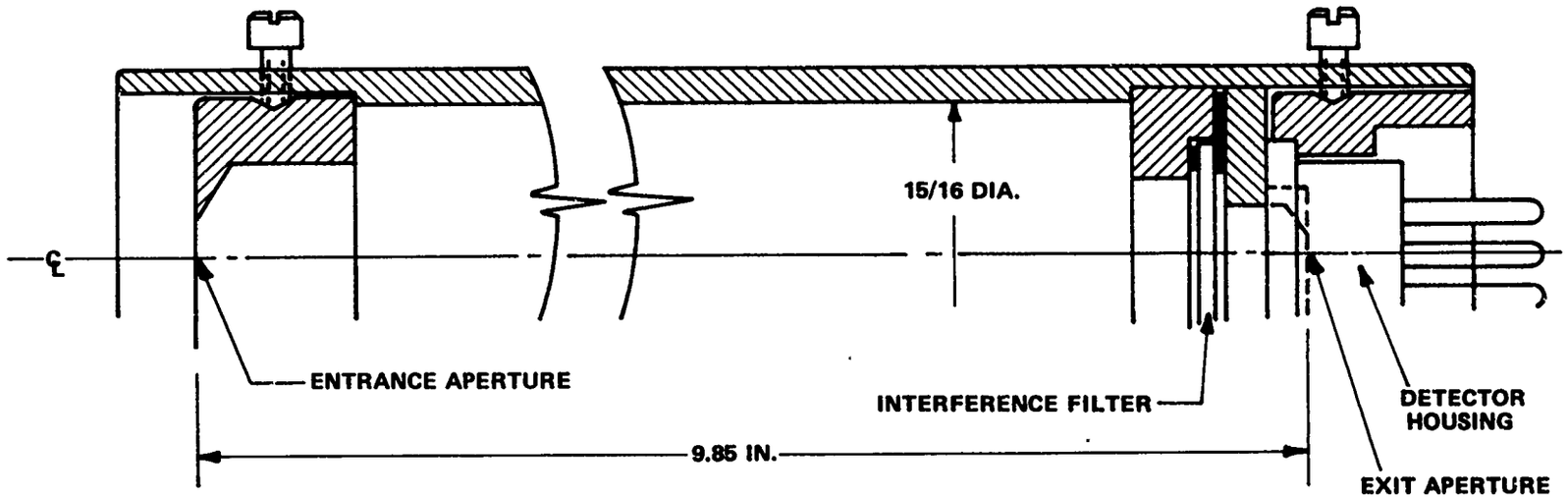

Figure A1 RADIOMETER DETAILS

band), which used an Eppley thermopile as the detector. The aperture at the entrance end was 6mm in diameter, and at the detector end it was slightly larger than the longest diagonal across the detector element, either .62 cm or .22 cm. Characteristics of the filters and detectors are given by Table AI.

Radiometers No. 1 through No. 5 were clustered in a bundle so that the radiation to each could be chopped by a common chopping wheel. They were installed in an enclosure along with No. 6 radiometer (which did not require chopping) so that temperature control necessary for instrument accuracy could be provided. This was done by mounting a fan blade outboard from the chopping wheel in its shadow so that there would be no interference with the chopping function. The fan served to draw a small flow of air through the enclosure. At the inlet, air was drawn over a heating coil that was thermostatically controlled for $\pm$ 2°F.

A sighting tube was fastened to the radiometer housing. This was used for aiming the radiometers, and it facilitated monitoring of their view of the flames.

Radiometer Calibration Apparatus

A schematic diagram of the apparatus used for calibration of radiometer components is shown in Figure A2. The infrared source was an electrically heated globar mounted in a baffled enclosure with an aperture about 3/8 in. diameter to expose the central portion of the globar. Radiation from this opening was directed along an optical path by a plane mirror near the opening to a concave mirror for focussing. Object distance was approximately equal to image distance. A motor-driven chopper was located near the image plane to modulate flux at 55 Hertz. The chopper exposed the detector over one-half its revolution. A filter wheel mount was located in front of the image plane, where the detector was placed.

The electric circuit for each detector was the same for calibration as for use during testing. The detector was connected in series with a battery

TABLE AI

RADIOMETER DETECTOR AND FILTER CHARACTERISTICS

Radiometer No.	1	2	3	4	5	6
Center Wavelength of Filter, microns	1.1	1.55	2.2	2.7	4.0	5.55
Peak Transmittance of Filter	0.58	0.64	0.74	0.87	0.80	0.60
Bandpass Half-Width, microns	0.10	0.20	0.45	0.68	0.36	0.55
Detector Type and Size, mm	PbS 4 x 4	PbS 4 x 4	PbS 1 x 1	PbS 1 x 1	PbSe 4 x 4	Thermo-pile, 10 dia
Specific Responsivity, cm^2/watt	180	220	250	100	1.6	$\frac{0.114\mu v}{\mu W\text{-}cm^2}$ *

*With CaF window in place.

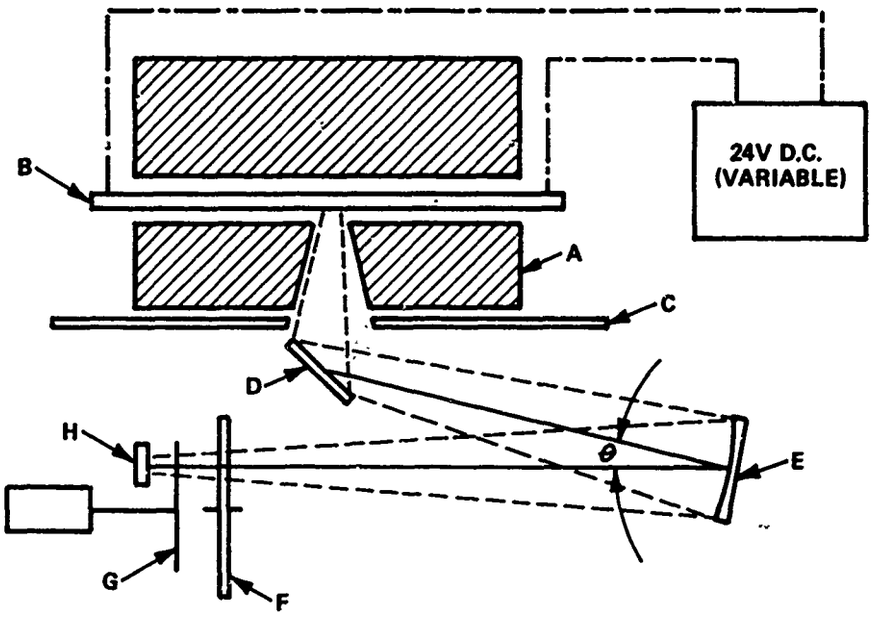

A - FIREBRICK ENCLOSURE
B - SILICON CARBIDE (GLOBAR) ROD
C - WATER-COOLED BAFFLE
D - FIRST-SURFACE TURNING MIRROR (PLANE)
E - 4.25" DIA., 9" FOCAL LENGTH SPHERICAL MIRROR
F - OPTICAL FILTER WHEEL
G - SECTORED-DISC BEAM CHOPPER
H - FOCAL PLANE (LOCATION OF THERMOPILE DETECTOR)

Figure A2 SCHEMATIC-ARRANGEMENT OF RADIOMETER CALIBRATION APPARATUS

to provide bias voltage. The circuit for each of four detectors was filtered and tapped for D. C. signal amplification to simplify recording, and the complete hookup is shown in Figure A3. It was necessary to use A. C. amplification for No. 5 radiometer, and its circuit is shown in Figure A4. The amplifiers for all circuits were mounted on a single chassis and could be adjusted for amplification factors of 1, 2, 5, 10, and 20. Output was recorded on a CEC Type 124 oscillograph using CEC Type 323 galvanometers. The thermopile that was used as a standard for comparison with detector output was made and calibrated by the Eppley Laboratory, Inc. of Newport, Rhode Island (Eppley No. 6359). It had been calibrated against a reference thermopile that had been standardized by comparing with an electrical compensation detector (Angstrom pyrheliometer) that had been calibrated in terms of the International Pyrheliometric Scale (1956). Accuracy of this standardization was claimed to be ± 2 percent. (1967 report to CAL, Inc. by Eppley Labs.) A Newport Type 307 amplifier was used to amplify the signal from the Eppley thermopile. Its circuit is shown by Figure A5. After using the thermopile for standardization, it was incorporated into No. 6 radiometer as its detector. One item of electrical apparatus used only during calibration was a digital microvoltmeter for indicating thermopile output.

Heat Meter Design

The heat meters that were used to indicate heat flux incident upon a surface near the fires were based upon the concept that the temperature difference between the center and the periphery of a thin wafer is proportional to incident heat transfer rate. The wafer must be supported in a relatively massive, cooled housing. Each wafer (.25 in. diameter, .015 in. thick) was made from constantan, and it was soldered into a narrow seat of a cylindrical copper body over one end of a hole that extended along the body centerline. Figure A6 shows the details. The meter thereby constituted a copper-constantan thermocouple, and with copper lead wires attached to the body and to the center of the wafer, its output emf was proportional to the radial temperature difference. This type heat meter has been shown to exhibit linearity of signal over a wide temperature range according to Ref. 10. Its sensitivity may be expressed by $E/q = 0.183 \frac{R^2}{S}$ mv/cal/cm^2-sec. for R and S in centimeters.

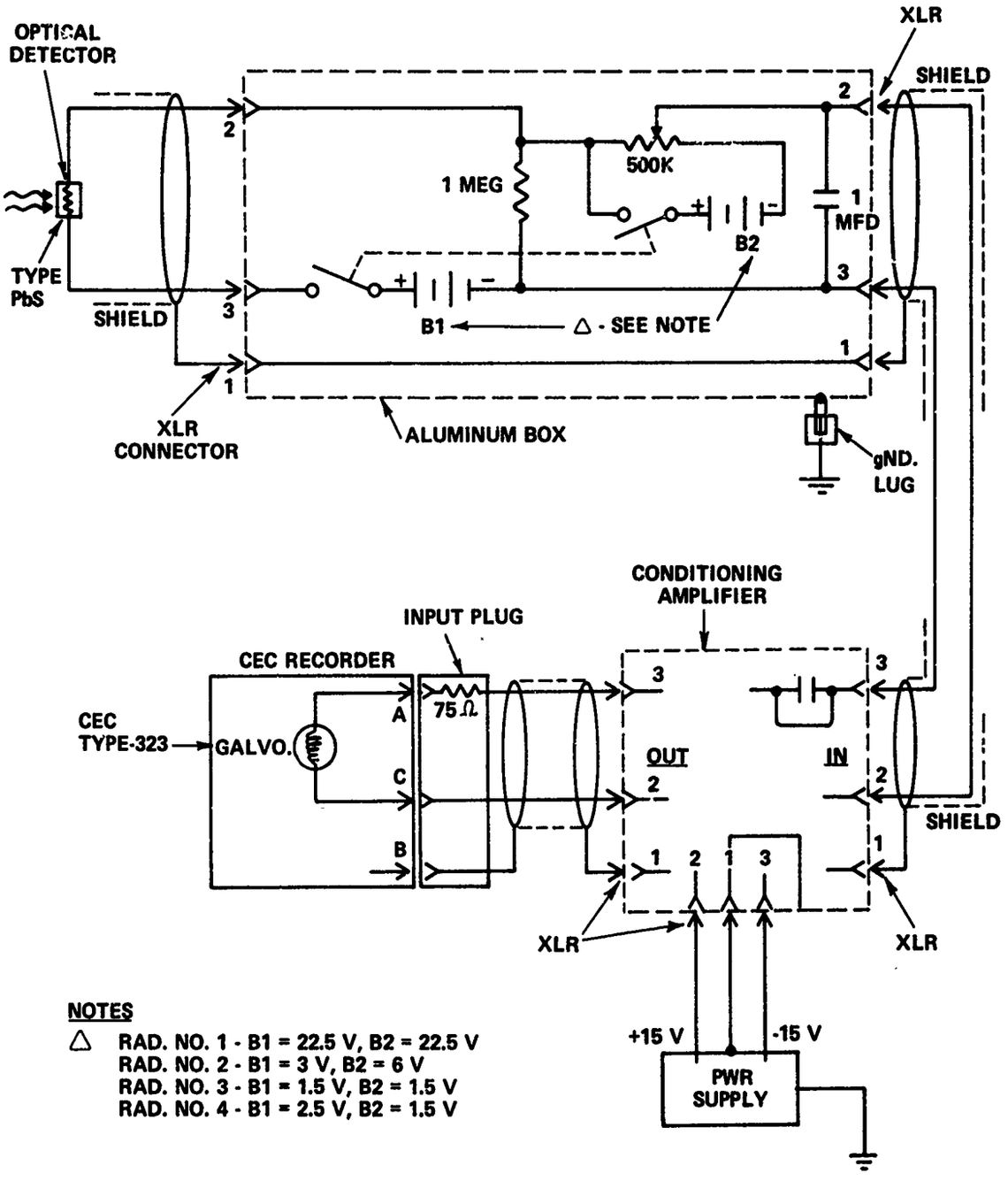

NOTES

△ RAD. NO. 1 - B1 = 22.5 V, B2 = 22.5 V
RAD. NO. 2 - B1 = 3 V, B2 = 6 V
RAD. NO. 3 - B1 = 1.5 V, B2 = 1.5 V
RAD. NO. 4 - B1 = 2.5 V, B2 = 1.5 V

Figure A3 RADIOMETER NO. 1 - NO. 4 SCHEMATIC

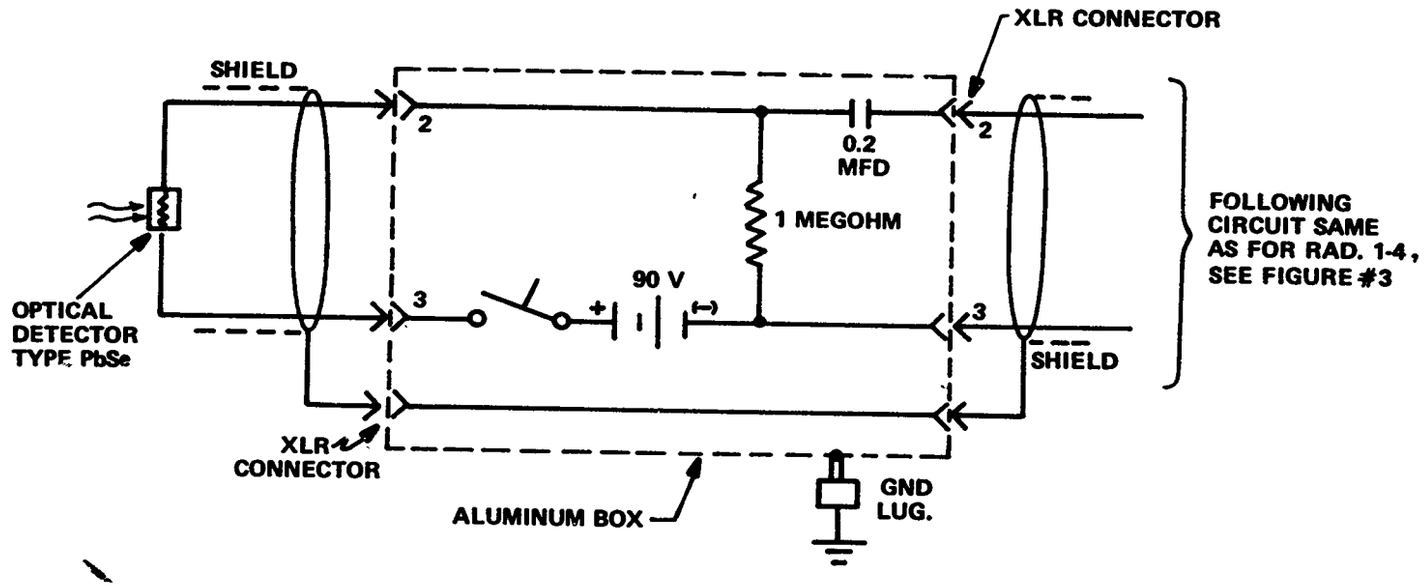

Figure A4 RADIOMETER NO. 5 SCHEMATIC

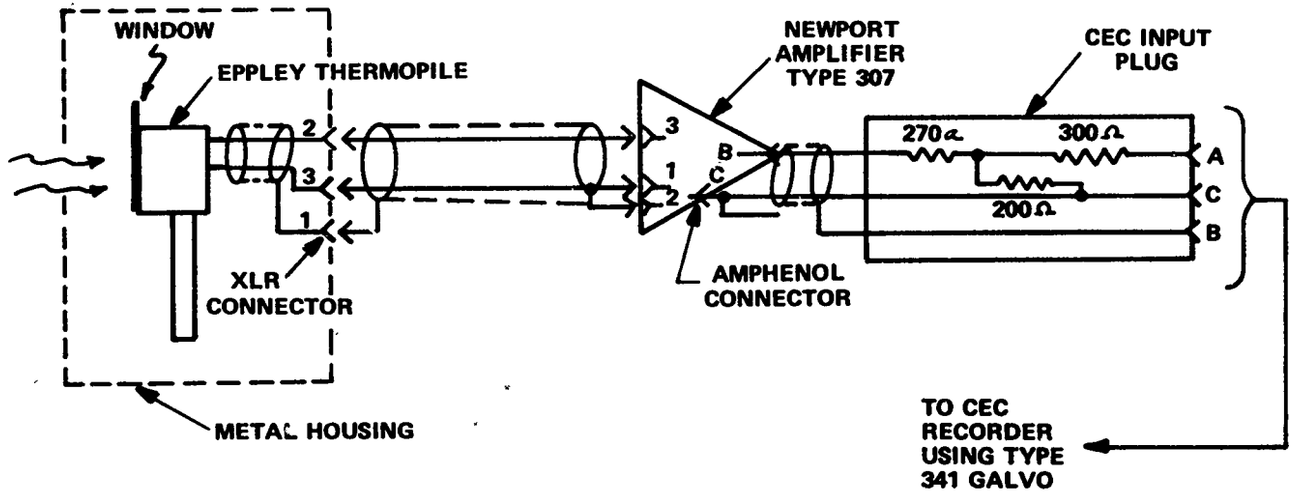

Figure A5 EPPLEY SCHEMATIC

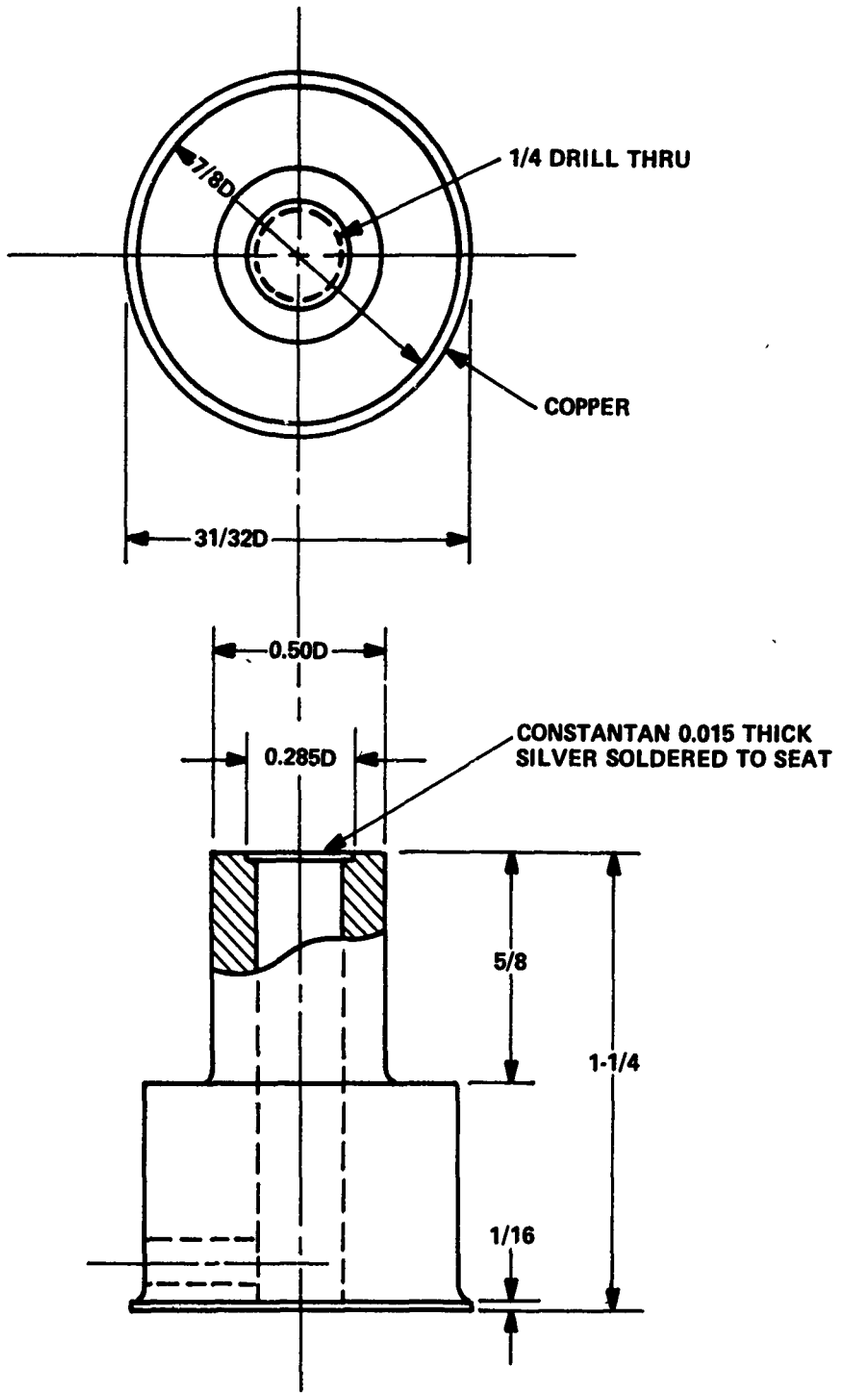

Figure A6 CONTINUOUS HEAT METER

Its speed of response may be expressed by a time constant, $\tau_0 = 3.7 R^2$ sec. The surface of each meter was coated with 3M Company "Velvet Black", which has an absorptivity of nearly unity.

The heat meters were calibrated to insure their accuracy. This was accomplished by recording meter output when it was placed on a hot copper slab at a fixed separation (.001 in.) between the slab surface and the constantan wafer. The procedure was to heat the slab by a Bunsen burner. The slab was taken out of the flame and the heat meter was placed upon it. The meter output was recorded on an L & N Speedomax AZAR recorder as was the output of a thermocouple in the copper slab. The meter was taken off the slab after a few seconds, and the slab was allowed to cool to a lower temperature. The procedure was repeated so that at least seven values of meter output were obtained over a slab temperature range of about 1200°F. The heat input to the meter was the sum of the radiant interchange and conduction through the air gap. This heat input was calculated from standard relations involving the temperatures of hot surface and the heat meter. The calibrations were checked periodically several times throughout the program and whenever a heat meter was exposed directly to fire.

During fire tests the emf from heat meters was recorded by a CEC oscillograph using Type 341 galvanometers. Seventy-five-ohm resistors were placed in series with the meters that were exposed to the most heat to reduce the sensitivity. The other meters were direct-connected to the common terminal box that was used for switching from a run mode to a calibration mode, whereby a known D. C. emf could be impressed for setting oscillograph deflections.

Fire Site and Arrangement of Instrumentation

The fire site was a level, flat concrete pad located within a heavy steel ring 12 ft. in diameter. The upper edge of the ring extended to a height 3 in. above the concrete so that a pool of liquid fuel could be contained. Two smaller rings were embedded in the concrete concentric with the 12 ft. ring.

Their edges also were at the 3 in. height, and their diameters were 3 and 6 ft. A larger pool was made (18 ft. 8 in. diameter) from a ring of 8 in. wide sheet steel which was partially sunk into the earth around the concrete pad.

The heat meters were arranged in four circles around the fire site. They were mounted on portable stands so that their elevation could be varied between 28 in. and 6 ft. above the ground, which was flat and level in the vicinity of the fire site. Eleven heat meters were fabricated with a stand for each. The three that were used for the positions nearest the fire were provided with water spray cooling at their base. This design resulted in a very small profile so that there would be no blocking of the view for instruments behind them. The rest of the heat meters were fixed to the side of 5-gallon pails (near the base) with epoxy cement, which were kept filled with water so they would not overheat during exposure to fire. The three that were placed in the second circle of meters around the site had their pails cut down to about a 5-in. height for reduced blocking of the view. All meters used copper lead wires, which were buried under a few inches of earth for protection near the fire site. Each stand was hollow so that lead wires were protected up to the meter. A 1/2 in. thick plate of Transite provided shielding of water pails from the fire, and each had a 5/8 in. diameter opening aligned with the heat meter which extended almost through it (to within 1/16 in. from the exposed surface).

The recording station was located 53 ft. from the 12 ft. ring in a westerly direction. Oscillographs were housed there along with power outlets, power supplies, and amplifiers for the radiometers. The radiometers were at an adjacent location. Two cameras, described below, were used. Both were located about 45 ft. from the fire. One was placed near the recording station, the other to the north of the fire site.

The soil at the fire site was the type classified as Ovid silt loam (new classification, Aeric Ochraqualfs, mixed Mesic.) This is a glacial till

mixed with reworked lake sediment. It has a high clay content (25 percent) and poor permeability (<0.2 in. of liquid/hr) in the naturally compacted state, Ref. 11.

A thermocouple stand was used during all fires after No. 4. It was located at the center of the site and supported four thermocouples at elevations of 11, 24, 36, and 47 in. A second stand was used during the larger fires. (12 and 18 ft. diameter pools). This stand was placed at the pool edge in the downwind direction, and it supported thermocouples at three elevations, 8, 18, and 70 in. All thermocouples were made from sheathed chromel-alumel wire (.040 in. sheath diameter) by baring the wires and spot welding to form a junction with exposed wires about 1/10 in. long. Wire size was 5 mils in diameter. The emf output from these thermocouples were recorded by oscillograph using direct-connected, Type 341 galvanometers.

Miscellaneous Apparatus

Two cameras were used for obtaining several still photographs during each fire. These were Hasselblad 500 EL models which used 120 film. Black-white type Tri-X was used for practically all fires, although the north camera used Ecktachrome during fires 19 to 23. Both cameras used 150mm focal length lenses for the 3 and 6 ft. diameter fires and 80mm lenses for the larger fires. Shutter speed was usually relatively fast (1/250 sec), and the aperture was set according to light meter readings taken at the camera location previous to the fire. Exposures ranging to several stops less were tried, but the pictures were found to lack detail even in the flame zone.

The instrument used for measuring wind velocity in the vicinity of the fire was a Flow Corporation (Cambridge, Massachusetts) hot wire anemometer, Model No. 55 B1.

Gas samples were analyzed using a Dräger gas detector manufactured by Drägerwerk, Lubeck, Germany. This detector consists of a hand-held

fixed displacement pump which draws the gas to be analyzed through a selected glass tube that is charged with chemicals and is expendable after each reading. After the proper amount of gas has been drawn through (as determined by the number of pump strokes specified for use of each tube type), the concentration of the gas to which the chemical is sensitive is indicated by length along the tube where a color change occurs. Each tube is properly scaled so that when the scale is read at the color change interface, the reading is obtained as concentration. A great variety of tubes are available so that many different gases can be detected. In addition, most are sensitive within a relatively small range of concentration in air. This makes it possible to obtain readings with good accuracy and to detect gases at very low levels of concentration.